MEASURABLE EUCLIDEAN RAMSEY THEORY FOR LINES AND FINITE CONFIGURATIONS

RYAN HOFF, GARY HU, AND YUMO LIU

Abstract. For finite configurations $X_1, \dots, X_r \subset \mathbb{E}^d$, write $\mathbb{E}^d \to_{\mathrm{m}} (X_1, \dots, X_r)$ when every measurable r-coloring of $\mathbb{E}^d$ contains an isometric copy of X_i in color i for some i. We extend Fourier-analytic and linear-programming methods for measurable distance-avoiding sets to this Euclidean Ramsey setting by combining finite inequalities for several color classes with spherical Fourier representations and positivity of the associated measures. This framework gives nine new measurable Euclidean Ramsey results for lines and finite configurations. Writing ℓ_m for the unit-spaced m-point line, we prove $\mathbb{E}^2 \to_{\mathrm{m}} (\ell_2, \ell_7)$, extending the planar positive result from ℓ_5 to a measurable result at ℓ_7. We further obtain new two- and three-color results for lines in several dimensions, new planar results for a regular pentagon and for a square of side length $\sqrt{2}$ with its center, and a measurable partial result toward the unresolved three-dimensional square problem: every measurable two-coloring of $\mathbb{E}^3$ contains either a monochromatic unit square or a monochromatic noncoplanar tetrahedron with four unit distances and two distances $\sqrt{2}$.

Contents

1. Introduction

Euclidean Ramsey theory, initiated in a series of papers by Erdős, Graham, Montgomery, Rothschild, Spencer, and Straus, asks which finite configurations are unavoidable in every coloring of Euclidean space [16, 17, 18]. For two configurations $X, Y \subset \mathbb{E}^d$, we write $\mathbb{E}^d \to (X, Y)$ if every red–blue coloring of $\mathbb{E}^d$ contains either a red X or a blue Y, up to isometry. Its negation, denoted $\mathbb{E}^d \not\to (X, Y)$, means that there exists a red–blue coloring with no red X and no blue Y. More generally, for finite configurations $X_1, \dots, X_r \subset \mathbb{E}^d$, write $\mathbb{E}^d \to (X_1, \dots, X_r)$ if every r-coloring of $\mathbb{E}^d$ contains an isometric copy of X_i in color i for some i. Thus $\mathbb{E}^d \not\to (X_1, \dots, X_r)$ means that there exists an r-coloring in which color i contains no copy of X_i for every i. We write $\to_{\mathrm{m}}$ when the color classes are required to be Lebesgue measurable. This restriction asks the question for a smaller class of colorings, but it also makes spatial averaging and Fourier analysis available: the indicator function of each color class can be averaged over large balls, and its Fourier transform controls averages of products at fixed distances. The arbitrary-coloring and measurable questions therefore have different strengths and different available methods.

We first discuss line configurations. For $m \geq 2$, let $\ell_m = \{0, 1, \dots, m-1\} \subset \mathbb{R}$ be the unit-spaced m-point line. Erdős, Graham, Montgomery, Rothschild, Spencer, and Straus proved $\mathbb{E}^2 \to (\ell_2, \ell_4)$ and, more generally, $\mathbb{E}^2 \to (\ell_2, K)$ for every three-point configuration $K \subset \mathbb{E}^2$ [17]. Tsaturian later proved $\mathbb{E}^2 \to (\ell_2, \ell_5)$ [30]. In dimension 3, Iván proved $\mathbb{E}^3 \to (\ell_2, K)$ for every five-point configuration $K \subset \mathbb{E}^3$, and Arman and Tsaturian proved $\mathbb{E}^3 \to (\ell_2, \ell_6)$ [21, 3]. On the other hand, Szlam proved that for some constant $c' > 0$, $\mathbb{E}^d \to (\ell_2, K)$ for every $K \subset \mathbb{E}^d$ with $|K| \leq 2^{c'd}$ [29]. In the opposite direction, Conlon and Fox proved $\mathbb{E}^2 \not\to (\ell_2, \ell_{10^{10}})$ and, for some constant $c > 0$, $\mathbb{E}^d \not\to (\ell_2, \ell_m)$ whenever $d \geq 2$ and $m \geq 2^{cd}$ [6]. Currier, Mody, Xie, and Zhang improved the planar obstruction to $\mathbb{E}^2 \not\to (\ell_2, \ell_{6330})$ [10]. The known planar results therefore leave the gap $6 \leq m \leq 6329$. We improve the lower bound in the measurable setting:

Theorem 1. $\mathbb{E}^2 \to_{\mathrm{m}} (\ell_2, \ell_7)$.

For three colors, the unit-distance graph of the plane is not 3-colorable by the Moser spindle, and hence $\mathbb{E}^2 \to (\ell_2, \ell_2, \ell_2)$ [25]. Currier, Moore, and Yip proved the three obstructions $\mathbb{E}^d \not\to (\ell_3, \ell_3, \ell_8)$, $\mathbb{E}^d \not\to (\ell_3, \ell_4, \ell_7)$, and $\mathbb{E}^d \not\to (\ell_3, \ell_5, \ell_5)$ for every $d \geq 2$ [12]. We prove a related result for three colors:

Theorem 2. $\mathbb{E}^2 \to_{\mathrm{m}} (\ell_2, \ell_2, \ell_3)$.

For two colors and red ℓ_3, Erdős, Graham, Montgomery, Rothschild, Spencer, and Straus proved $\mathbb{E}^3 \to (K, K)$ for every three-point configuration $K \subset \mathbb{E}^3$, and hence $\mathbb{E}^3 \to (\ell_3, \ell_3)$ [16]. Currier, Moore, and Yip later proved the positive planar result $\mathbb{E}^2 \to (\ell_3, \ell_3)$ with computer assistance [11]. Conlon and Wu proved $\mathbb{E}^d \not\to (\ell_3, \ell_{10^{50}})$ for every $d \geq 2$ [8]. Führer and Tóth improved 10^{50} to 1177 [19], and Currier, Moore, and Yip later improved it to 20 [12]. Thus, in the plane, there remains a gap $4 \leq m \leq 19$. We prove three results for measurable colorings in higher dimensions. The dimensions in these statements record where the present constructions work. We do not claim that they are optimal.

Theorem 3. $\mathbb{E}^3 \to_{\mathrm{m}} (\ell_3, \ell_4)$.

Theorem 4. $\mathbb{E}^4 \to_{\mathrm{m}} (\ell_3, \ell_5)$.

Theorem 5. $\mathbb{E}^7 \to_{\mathrm{m}} (\ell_3, \ell_6)$.

For red ℓ_4, Erdős, Graham, Montgomery, Rothschild, Spencer, and Straus proved $\mathbb{E}^d \nrightarrow (\ell_6, \ell_6)$ and $\mathbb{E}^d \nrightarrow (\ell_4, \ell_4, \ell_4)$ for every $d \geq 2$ [16]. For two colors, interchanging the colors in $\mathbb{E}^2 \to (\ell_2, \ell_4)$ gives $\mathbb{E}^2 \to (\ell_4, \ell_2)$ [17]. Currier, Moore, and Yip proved $\mathbb{E}^d \nrightarrow (\ell_4, \ell_{14})$ and $\mathbb{E}^d \nrightarrow (\ell_5, \ell_8)$ for every $d \geq 2$ [12]. Thus the planar gap for red ℓ_4 is $3 \leq m \leq 13$. In a higher dimension we prove a result for measurable colorings:

Theorem 6. $\mathbb{E}^4 \to_{\mathrm{m}} (\ell_4, \ell_4)$.

More generally, Conlon and Führer proved that if a finite configuration $X \subset \mathbb{E}^d$ is not contained in a sphere, then there is an integer m such that $\mathbb{E}^n \nrightarrow (X, \ell_m)$ for every $n \geq d$ [7].

We next turn to finite point configurations. For $n \geq 3$, let P_n be the regular n-gon of side length one. For $s > 0$, let $W_n(s)$ be a regular n-gon of side length s together with its center. In particular, $W_4(\sqrt{2})$ is a square of side length $\sqrt{2}$ together with its center.

Juhász proved that $\mathbb{E}^2 \to (\ell_2, K)$ for every four-point configuration $K \subset \mathbb{E}^2$, and in the same paper gave a twelve-point configuration $K \subset \mathbb{E}^2$ with $\mathbb{E}^2 \nrightarrow (\ell_2, K)$ [23]. Csizmadia and Tóth later reduced the size of such an obstruction to eight: $\mathbb{E}^2 \nrightarrow \left(\ell_2, W_7(\frac{9}{5}\sin(\pi/7))\right)$ [9]. Thus $\mathbb{E}^2 \to (\ell_2, W_3(s))$ for every $s > 0$, while the corresponding statement fails for $W_7(\frac{9}{5}\sin(\pi/7))$. This leaves a gap which we partially close in the measurable setting:

Theorem 7. $\mathbb{E}^2 \to_{\mathrm{m}} (\ell_2, W_4(\sqrt{2}))$.

For regular polygons, the preceding four-point theorem gives $\mathbb{E}^2 \to (\ell_2, P_4)$. Currier, Mody, Xie, and Zhang proved that if $K \subset \mathbb{E}^n$ is 1-separated, $R_K > 2$, and $\operatorname{diam}(K) \leq R_K - 1$, then $|K| \gtrsim (11 + o(1))^n \ln R_K$ implies $\mathbb{E}^n \nrightarrow (\ell_2, K)$. If K is contained in an affine subspace of dimension at most $(\ln 5/\ln 11)n$, the factor $11 + o(1)$ can be replaced by $5 + o(1)$ [10]. Applying that construction to regular polygons and carrying out the explicit calculation in Proposition 43 gives $\mathbb{E}^2 \nrightarrow (\ell_2, P_N)$ for every integer $N \geq 6800$. The case P_6 is elementary and needs no measurability. The remaining case immediately beyond P_4 is P_5. Under the measurable hypothesis we prove:

Theorem 8. $\mathbb{E}^2 \to_{\mathrm{m}} (\ell_2, P_5)$.

If e_1, e_2, e_3 are orthonormal, set $\mathcal{S} = \{0, e_1, e_2, e_1 + e_2\}$ and $\mathcal{T} = \left\{0, e_1, e_2, \frac{1}{2}e_1 + \frac{\sqrt{3}}{2}e_3\right\}$. Thus $\mathcal{S}$ is a unit square and $\mathcal{T}$ is a noncoplanar tetrahedron with four distances 1 and two distances $\sqrt{2}$.

For the final configuration, a folklore construction gives a two-coloring of $\mathbb{E}^2$ with no monochromatic copy of $\mathcal{S}$, that is, $\mathbb{E}^2 \nrightarrow (\mathcal{S}, \mathcal{S})$. See Gasarch, Gezalyan, and Parker [20]. Erdős, Graham, Montgomery, Rothschild, Spencer, and Straus proved $\mathbb{E}^6 \to (\mathcal{S}, \mathcal{S})$ [16]. As Cantwell notes, a trivial modification of their proof gives $\mathbb{E}^5 \to (\mathcal{S}, \mathcal{S})$ [5]. Cantwell later proved $\mathbb{E}^4 \to (\mathcal{S}, \mathcal{S})$ for arbitrary colorings [5]. Thus $\mathbb{E}^d \to (\mathcal{S}, \mathcal{S})$ is known for every $d \geq 4$. Dimension 3 remains open, while dimension 2 is ruled out by the coloring above. We address this missing dimension with the following measurable result. Up to isometry, four points with four mutual distances equal to 1 and two equal to $\sqrt{2}$ form either a square, when the two $\sqrt{2}$-pairs are disjoint, or the noncoplanar tetrahedron $\mathcal{T}$, when the two pairs share a vertex. We prove that one of these two configurations must occur monochromatically:

Theorem 9. *Every measurable two-coloring of* $\mathbb{E}^3$ *contains a monochromatic copy of either* $\mathcal{S}$ *or* $\mathcal{T}$*.*

The nine results play different roles. Theorem 1 extends the planar positive results from ℓ_5 to a measurable result at ℓ_7, while Theorem 2 gives a three-color analogue. The higher-dimensional line theorems show that the same method applies beyond the planar setting. Theorem 7 begins to close the gap for regular polygons with their centers, while Theorem 8 gives the corresponding measurable result for the regular pentagon. Theorem 9 gives a measurable partial result toward the unresolved three-dimensional square problem.

Our method extends the Fourier-analytic and linear-programming approach to measurable distance-avoiding sets, initiated by Székely and developed by de Oliveira Filho and Vallentin [28, 14]. Related work treats finite unit-distance constraints, correlations involving three or more points, and more general optimization problems [4, 24, 1, 2, 13].

The spherical Fourier representation and the positivity of the associated measures are standard ingredients in measurable distance-avoidance arguments. Here we combine them with finite inequalities for Ramsey statements in which different color classes are subject to different avoidance conditions. In the planar arguments, these inequalities involve several color indicators at once. In higher dimensions, we organize the possible local color patterns into a finite directed graph. Assigning a number to each vertex makes the intermediate terms cancel when the local inequalities are added along a line. This gives one method for treating all of the results below.

Our three-color result gives a simple example of the argument. Call the three colors red, blue, and green, and consider the 3×3 triangular-lattice patch used to prove Theorem 2. Suppose that this patch contains neither a red pair nor a blue pair at distance one, and no green copy of ℓ_3. We assign coefficients to the points and to pairs of points at the distances appearing in the patch. The resulting quadratic functional $\mathcal{L}$ is chosen so that every coloring of the patch with these avoidance properties satisfies $\mathcal{L} \geq 0$. The linear terms record the colors of individual points, and the quadratic terms record pairs of points with prescribed colors.

Now place this patch at all translations and rotations and average $\mathcal{L}$ over a large ball. The boundary contribution tends to zero as the ball grows. The remaining terms are color densities and pair correlations at the finitely many distances in the patch. After the densities are subtracted from the indicator functions, Fourier analysis writes each correlation as an integral against a nonnegative measure. The integrand is a finite linear combination of spherical averages determined by the distances in the patch. A pointwise upper bound for this integrand therefore gives an upper bound for the averaged value of $\mathcal{L}$. In the nine-point case this upper bound is negative, contradicting the nonnegative lower bound obtained from every coloring of the patch. The coefficients are chosen so that the local expression is nonnegative while the associated polynomial in the color density and kernel bound give a negative average. This links the finite combinatorial inequality to the Fourier estimate for its average.

The other planar results use the same argument with different patches, quadratic expressions, and coefficients. For the line results, a possible coloring of a short sequence of consecutive points is treated as a local pattern. Appending one new point shifts the sequence by one place and gives a directed edge between two allowed patterns. Assign a number $\phi(u)$ to each pattern u. If the edge from u to v has contribution $W(u, v)$, the local inequalities take the form $W(u, v) + \phi(u) - \phi(v) \geq 0$. Summing these inequalities along an oriented line makes the intermediate ϕ-terms cancel and leaves only contributions from the two ends. This is the line analogue of the finite-patch inequality. For $W_4(\sqrt{2})$, P_5, and the square–tetrahedron result, the patch is instead a finite point set containing copies of the configurations under consideration.

The planar and line averaging propositions later in the paper separate the finite lower bound, the averaged upper bound, and the boundary error in these two forms of the argument.

The coefficients are found by linear programs whose constraints encode the finite colorings of the patch and the desired bounds for the Fourier kernels at selected frequencies. The linear programs are used to find the coefficients. The proofs use rounded rational or integer values, check the local inequalities directly, and establish the kernel bounds analytically over the full frequency range. Measurability enters at the averaging step: it makes the color indicators measurable and supplies the spatial averages and Fourier representations used above. Without it, these analytic quantities need not be available.

The paper is organized as follows. Section 2 develops the spherical averaging estimates. Sections 3–8 prove the nine Ramsey theorems. Section 9 describes the linear programs, and Section 10 gives finite-radius consequences, the explicit polygon obstruction, and open problems. The appendices record the finite data and the rational verifications used in the proofs.

2. Fourier averaging

2.1. **Spherical averaging.** Let $d \geq 2$ and let $B_T = \{x \in \mathbb{R}^d : |x| \leq T\}$ be the closed Euclidean ball of radius T centered at the origin. We use $|B_T|$ for its volume. Let $h : \mathbb{R}^d \to \mathbb{R}$ be bounded and measurable, and let $h_T = h\mathbf{1}_{B_T}$ be its restriction to B_T. Thus h_T is zero outside the ball.

Let σ_{d-1} be surface measure on the unit sphere $\mathbb{S}^{d-1}$ divided by the total surface area, so that $\sigma_{d-1}(\mathbb{S}^{d-1}) = 1$. For $\omega \in \mathbb{S}^{d-1}$, write ω_1 for its first coordinate.

For $r \geq 0$, define the spherical autocorrelation of h_T at distance r by

$$\mathcal{A}_{h,T}(r) = \frac{1}{|B_T|} \int_{\mathbb{S}^{d-1}} \int_{\mathbb{R}^d} h_T(y) h_T(y + r\omega) \, \mathrm{d}y \, \mathrm{d}\sigma_{d-1}(\omega),$$

The product compares the values of h_T at two points whose displacement is $r\omega$. The outer integral averages over all directions of that displacement. The factor $|B_T|^{-1}$ normalizes the average by the volume of the ball. The truncation to B_T makes all these integrals finite.

We next express this correlation in terms of the Fourier transform. We use the unitary convention

$$\widehat{f}(\xi) = \frac{1}{(2\pi)^{d/2}} \int_{\mathbb{R}^d} e^{-i\xi\cdot x} f(x)\,\mathrm{d}x,$$

for which Plancherel's identity has no additional constant [27, Eq. (6.5.1), Theorem 6.5.6, and Eq. (6.5.33)]. The vector ξ is the Fourier frequency: it records the oscillation of the function $x \mapsto e^{i\xi\cdot x}$. For $a \in \mathbb{R}^d$, Plancherel's identity and the Fourier transform of a translate gives

$$\int_{\mathbb{R}^d} h_T(y)h_T(y+a)\,\mathrm{d}y = \int_{\mathbb{R}^d} e^{-i\xi\cdot a}|\widehat{h_T}(\xi)|^2\,\mathrm{d}\xi.$$

The complex exponential is the factor by which the Fourier component at frequency ξ changes under translation by a.

Plancherel gives $\int_{\mathbb{R}^d} |\widehat{h_T}(\xi)|^2\,\mathrm{d}\xi = \int_{B_T} |h(x)|^2\,\mathrm{d}x < \infty$. Define the resulting finite nonnegative measure $\widehat{\nu}_{h,T}$ on $\mathbb{R}^d$ by

$$\mathrm{d}\widehat{\nu}_{h,T}(\xi) = \frac{|\widehat{h_T}(\xi)|^2}{|B_T|}\,\mathrm{d}\xi.$$

It is nonnegative because its density is nonnegative. Let $\nu_{h,T}$ be the measure on $[0,\infty)$ obtained by recording only the length of the frequency: for every Borel set $B \subset [0,\infty)$, $\nu_{h,T}(B) = \widehat{\nu}_{h,T}(\{\xi : |\xi| \in B\})$. Thus the variable t below is the magnitude $|\xi|$ of a Fourier frequency. The measure changes with T because h_T changes with T, but t always ranges over $[0,\infty)$ and has this same meaning. From this point on, $\nu_{h,T}$ denotes a measure on Fourier radii of this kind, while μ is reserved for the centered red-indicator measure defined below.

When $a = r\omega$ and we average over all directions ω, rotational invariance shows that the average of $e^{-i\xi\cdot a}$ depends only on the product $r|\xi|$. We denote this one-variable function

$$\Omega_d(u) = \int_{\mathbb{S}^{d-1}} e^{-iu\omega_1}\,\mathrm{d}\sigma_{d-1}(\omega).$$

Therefore

$$\int_{\mathbb{S}^{d-1}} e^{-ir\xi\cdot\omega}\,\mathrm{d}\sigma_{d-1}(\omega) = \Omega_d(r|\xi|),$$

because, when $\xi \neq 0$, a rotation carries $\xi/|\xi|$ to the first coordinate vector. When $\xi = 0$, both sides are 1. The function Ω_d is real and even by symmetry, and $\Omega_d(0) = 1$ because σ_{d-1} is a probability measure.

For $\alpha \geq 0$ and $t \geq 0$, let Γ denote the gamma function and let J_α be the Bessel function of the first kind with parameter α, defined by

$$J_\alpha(t) = \sum_{n=0}^{\infty} \frac{(-1)^n}{n!\,\Gamma(n+\alpha+1)} \left(\frac{t}{2}\right)^{2n+\alpha}.$$

The series converges for every t, and in particular $J_0(t) = \sum_{n=0}^{\infty}(-1)^n(t^2/4)^n/(n!)^2$.

Lemma 10. *Let $d \geq 2$. For $t > 0$,*

$$\Omega_d(t) = \Gamma\left(\frac{d}{2}\right)\left(\frac{2}{t}\right)^{d/2-1} J_{d/2-1}(t) = \sum_{n=0}^{\infty} \frac{(-1)^n t^{2n}}{2^n n!\, d(d+2)\cdots(d+2n-2)},$$

where $J_{d/2-1}$ is the Bessel function of the first kind with parameter $d/2-1$, and the product in the denominator is 1 when $n=0$. Moreover, for every $t \in \mathbb{R}$,

$$|\Omega_d'(t)| \le \frac{2\Gamma(d/2)}{(d-1)\sqrt{\pi}\,\Gamma((d-1)/2)}.$$

Proof. The Bessel representation is the spherical Fourier-transform formula [14, Eq. (1)]. Substituting the power series for $J_{d/2-1}$ [26, Eq. 10.2.2] and simplifying the gamma factors gives, with $\alpha = d/2-1$,

$$\Gamma\left(\frac{d}{2}\right)\left(\frac{2}{t}\right)^{\alpha} \frac{(-1)^n t^{2n+\alpha}}{2^{2n+\alpha} n!\,\Gamma(n+d/2)} = \frac{(-1)^n t^{2n}}{2^n n! \prod_{j=0}^{n-1}(d+2j)},$$

which is the series above.

For the derivative estimate, dominated convergence applies because $|\partial_t e^{-it\omega_1}| = |\omega_1| \le 1$. Therefore

$$\Omega_d'(t) = -i\int_{\mathbb{S}^{d-1}} \omega_1 e^{-it\omega_1}\,\mathrm{d}\sigma_{d-1}(\omega),$$

so $|\Omega_d'(t)|$ is at most the mean of $|\omega_1|$ on the sphere. The first coordinate of a uniformly distributed point of $\mathbb{S}^{d-1}$ has density

$$\frac{\Gamma(d/2)}{\sqrt{\pi}\,\Gamma((d-1)/2)}(1-u^2)^{(d-3)/2}$$

on $[-1,1]$ [15, Remark 2.10]. Consequently,

$$\begin{aligned}\int_{\mathbb{S}^{d-1}} |\omega_1|\,\mathrm{d}\sigma_{d-1}(\omega) &= \frac{2\Gamma(d/2)}{\sqrt{\pi}\,\Gamma((d-1)/2)}\int_0^1 u(1-u^2)^{(d-3)/2}\,\mathrm{d}u \\ &= \frac{2\Gamma(d/2)}{(d-1)\sqrt{\pi}\,\Gamma((d-1)/2)}.\end{aligned}$$

With $v = 1-u^2$ and $dv = -2u\,du$, one has

$$\int_0^1 u(1-u^2)^{(d-3)/2}\,\mathrm{d}u = \frac{1}{2}\int_0^1 v^{(d-3)/2}\,\mathrm{d}v = \frac{1}{d-1},$$

which gives the final equality. ☐

The cases needed below are

$$\Omega_2(t) = J_0(t), \qquad \Omega_3(t) = \frac{\sin t}{t},$$
$$\Omega_4(t) = \frac{2J_1(t)}{t}, \qquad \Omega_7(t) = 15\frac{(3-t^2)\sin t - 3t\cos t}{t^5}.$$

Each expression has value 1 at $t=0$ by continuity. These formulas follow from the preceding lemma and the standard half-integer formulas for $J_{1/2}$ and $J_{5/2}$ [26, Eq. (10.47.3) and Sec. 10.49(i)].

Lemma 11. *Let $\nu_{h,T}$ be the measure on Fourier radii obtained from $\widehat{\nu}_{h,T}$ by mapping ξ to $|\xi|$. Then, for every $r \ge 0$,*

$$\mathcal{A}_{h,T}(r) = \int_0^\infty \Omega_d(rt)\,\mathrm{d}\nu_{h,T}(t).$$

Moreover,

$$\nu_{h,T}([0,\infty)) = \frac{1}{|B_T|}\int_{B_T} h(x)^2\,\mathrm{d}x.$$

Thus $\nu_{h,T}$ *has mass* $|B_T|^{-1}\|h_T\|_2^2$.

Proof. This is the spherical autocorrelation identity from [14, Sec. 2]. We give the proof to fix the normalization. Since $h_T \in L^2(\mathbb{R}^d)$ is real-valued, Plancherel's identity and the Fourier transform of a translate give, for every $a \in \mathbb{R}^d$,

$$\int_{\mathbb{R}^d} h_T(y)h_T(y+a)\,\mathrm{d}y = \int_{\mathbb{R}^d} e^{-i\xi\cdot a}|\widehat{h_T}(\xi)|^2\,\mathrm{d}\xi.$$

Set $a = r\omega$ and average over $\omega \in \mathbb{S}^{d-1}$. Fubini's theorem applies because $|\widehat{h_T}|^2$ is integrable. Rotational invariance and the definition of Ω_d give

$$\int_{\mathbb{S}^{d-1}} e^{-ir\xi\cdot\omega}\,\mathrm{d}\sigma_{d-1}(\omega) = \Omega_d(r|\xi|).$$

Grouping the integral according to the value $t = |\xi|$, which is the definition of $\nu_{h,T}$, gives

$$\frac{1}{|B_T|}\int_{\mathbb{R}^d} \Omega_d(r|\xi|)|\widehat{h_T}(\xi)|^2\,\mathrm{d}\xi = \int_0^\infty \Omega_d(rt)\,\mathrm{d}\nu_{h,T}(t).$$

Finally, Plancherel's identity gives

$$\nu_{h,T}([0,\infty)) = \frac{1}{|B_T|}\int_{\mathbb{R}^d} |\widehat{h_T}(\xi)|^2\,\mathrm{d}\xi = \frac{1}{|B_T|}\int_{B_T} h(x)^2\,\mathrm{d}x.$$

□

The measure $\nu_{h,T}$ is nonnegative, so an upper or lower bound for the function multiplying it in the integral gives the corresponding bound after the total mass of the measure is known. We call that multiplying function the kernel. In dimension two, write $\omega = (\cos\theta, \sin\theta)$ and let ρ_θ denote rotation through θ. Since $\Omega_2 = J_0$, the kernel associated with two points at distance r is $J_0(rt)$.

2.2. **Truncation estimates.** Lemma 11 integrates over all of $\mathbb{R}^d$, whereas our averages are taken over B_T. The difference is confined to a boundary region whose relative volume tends to zero: if $a \in \mathbb{R}^d$ is fixed and $T > |a|$, then $B_T \triangle (B_T + a)$, the set of points belonging to one of the two balls, is contained in $B_{T+|a|} \setminus B_{T-|a|}$. Hence

$$|B_T \triangle (B_T + a)| = O(T^{d-1}). \tag{2.1}$$

The containing annulus has volume $O(T^{d-1})$ for fixed a, since $|B_r| = |B_1|r^d$. Here and below, the constants implicit in $O(T^{-1})$ may depend on the fixed distances, the dimension, and the bound for the function, but not on T.

For quantitative statements, put $D_d = d2^d$. If $T \geq k \geq 0$ and $|a| = k$, then

$$\frac{|B_T \triangle (B_T + a)|}{|B_T|} \leq \frac{(T+k)^d - (T-k)^d}{T^d} \leq \frac{D_d k}{T}. \tag{2.2}$$

The last inequality follows from the mean value theorem and $T + k \leq 2T$.

For a bounded measurable $f : \mathbb{R}^d \to \mathbb{R}$, define its average on B_T by $p_T(f) = |B_T|^{-1}\int_{B_T} f(x)\,\mathrm{d}x$. When f is an indicator function, $p_T(f)$ is the proportion of the corresponding set in B_T. For $k \geq 0$, define the finite-ball spherical two-point correlation at distance k by

$$C_{k,T}(f) = \frac{1}{|B_T|} \int_{\mathbb{S}^{d-1}} \int_{B_T} f(x) f(x + k\omega)\, \mathrm{d}x\, \mathrm{d}\sigma_{d-1}(\omega).$$

Thus p_T records a one-point average, whereas $C_{k,T}$ records a two-point correlation. The quantity $\mathcal{A}_{h,T}$ above is the whole-space autocorrelation of the truncated function h_T. The estimates below compare $C_{k,T}(f)$ with this Fourier-analytic quantity. For a fixed function, we abbreviate these quantities to p_T and $C_{k,T}$.

Lemma 12. *Let $f : \mathbb{R}^d \to \mathbb{R}$ be bounded and measurable. The following estimates hold.*

(i) For fixed $k \geq 0$,

$$C_{k,T}(f) = \int_0^\infty \Omega_d(kt)\, \mathrm{d}\nu_{f,T}(t) + O(T^{-1}).$$

If $T \geq k$ and $B = \|f\|_\infty$, the error has absolute value at most $B^2 D_d k/T$.

(ii) For $m \geq 1$, let $\phi : \mathbb{R}^m \to \mathbb{R}$ be measurable and bounded on $[-\|f\|_\infty, \|f\|_\infty]^m$. The average over $x \in B_T$ and $\omega \in \mathbb{S}^{d-1}$ of

$$\phi(f(x), \ldots, f(x + (m-1)\omega)) - \phi(f(x+\omega), \ldots, f(x + m\omega))$$

is $O(T^{-1})$. If $T \geq 1$ and M_ϕ is the supremum of $|\phi|$ on this cube, the absolute value of this average is at most $M_\phi D_d/T$.

Proof. (i) For a fixed ω, the autocorrelation of the truncation $f\mathbf{1}_{B_T}$ is

$$\int_{\mathbb{R}^d} (f\mathbf{1}_{B_T})(x)(f\mathbf{1}_{B_T})(x + k\omega)\, \mathrm{d}x = \int_{B_T \cap (B_T - k\omega)} f(x) f(x + k\omega)\, \mathrm{d}x.$$

The two domains being compared are $B_T \cap (B_T - k\omega)$ and B_T, respectively. The absolute difference is at most $B^2|B_T \triangle (B_T - k\omega)|$. Averaging over ω, dividing by $|B_T|$, applying (2.2), and then using Lemma 11 prove both the first formula and its explicit error bound.

(ii) For the second statement, put $\Phi(x, \omega) = \phi(f(x), \ldots, f(x + (m-1)\omega))$. The stated average is

$$\frac{1}{|B_T|} \int_{\mathbb{S}^{d-1}} \int_{B_T} \Big(\Phi(x, \omega) - \Phi(x + \omega, \omega)\Big)\, \mathrm{d}x\, \mathrm{d}\sigma_{d-1}(\omega).$$

For fixed ω, the substitution $y = x + \omega$ gives

$$\int_{B_T} \Phi(x + \omega, \omega)\, \mathrm{d}x = \int_{B_T + \omega} \Phi(y, \omega)\, \mathrm{d}y.$$

Thus the absolute difference between the two integrals is at most $M_\phi |B_T \triangle (B_T + \omega)|$, uniformly in ω. After the translation, both integrals have the same integrand $\Phi(\cdot, \omega)$, so their difference is supported only on the symmetric difference of the two domains. Averaging, dividing by $|B_T|$, and applying (2.2) with $k = 1$ proves the claim and its explicit bound.

$\square$

Lemma 13. *In dimension two, let $h : \mathbb{R}^2 \to [-1,1]$ be measurable, let $p, q \in \mathbb{R}^2$, put $M = \max\{|p|, |q|\}$, and suppose $T > 2M$. Then the following two estimates hold, where $\nu_{h,T}$ is the measure on Fourier radii obtained from the measure*

$$\mathrm{d}\widehat{\nu}_{h,T}(\xi) = \frac{|\widehat{h_T}(\xi)|^2}{|B_T|}\,\mathrm{d}\xi$$

defined above:

(i)

$$\left| \frac{1}{2\pi|B_T|} \int_0^{2\pi} \int_{B_T} h(x + \rho_\theta p)\,\mathrm{d}x\,\mathrm{d}\theta - p_T(h) \right| \le \frac{4M}{T}, \tag{2.3}$$

(ii)

$$\left| \frac{1}{2\pi|B_T|} \int_0^{2\pi} \int_{B_T} h(x + \rho_\theta p) h(x + \rho_\theta q)\,\mathrm{d}x\,\mathrm{d}\theta - \int_0^\infty J_0(|p-q|t)\,\mathrm{d}\nu_{h,T}(t) \right| \le \frac{12M}{T}. \tag{2.4}$$

Proof. (i) If $a \in \mathbb{R}^2$ and $|a| < T$, then the annulus estimate is

$$|B_T \triangle (B_T + a)| \le \pi(T + |a|)^2 - \pi(T - |a|)^2 = 4\pi T|a|.$$

For (2.3), substitute $y = x + \rho_\theta p$. The domains $B_T + \rho_\theta p$ and B_T have symmetric difference of area at most $4\pi T|p| \le 4\pi TM$. Since $|h| \le 1$, this bounds the difference of the corresponding integrals. Averaging over θ and dividing by $|B_T| = \pi T^2$ gives (2.3).

(ii) For (2.4), put $w_\theta = \rho_\theta(q - p)$ and again substitute $y = x + \rho_\theta p$. The inner integral becomes

$$\int_{B_T + \rho_\theta p} h(y) h(y + w_\theta)\,\mathrm{d}y,$$

whereas the truncated autocorrelation is

$$\int_{\mathbb{R}^2} h_T(y) h_T(y + w_\theta)\,\mathrm{d}y = \int_{B_T \cap (B_T - w_\theta)} h(y) h(y + w_\theta)\,\mathrm{d}y.$$

The integrand has absolute value at most 1. By the triangle inequality for symmetric differences, the difference of the two integrals is therefore at most

$$|B_T \triangle (B_T + \rho_\theta p)| + |B_T \triangle (B_T - w_\theta)| \le 4\pi T|p| + 4\pi T|w_\theta|.$$

Since $|w_\theta| = |q - p| \le 2M$, the last expression is at most $12\pi TM$. This bound is the source of the factor $12M/T$: after averaging and dividing by πT^2, the error is at most $12M/T$. As θ varies uniformly, w_θ varies uniformly over the circle of radius $|p - q|$. Lemma 11 and $\Omega_2 = J_0$ identify its truncated autocorrelation with the integral in (2.4).

□

For indicator functions, subtracting the average separates the constant term from the remaining correlation. This gives the form used in the higher-dimensional proofs.

Lemma 14. *Let $r : \mathbb{R}^d \to \{0,1\}$ be measurable, put $p = p_T(r)$, and define the T-dependent centered function*

$$f_T = r - p_T(r).$$

Let $\mu_{f,T}$ be the measure on Fourier radii associated with the centered function $f_T\mathbf{1}_{B_T}$. Then $\mu_{f,T}$ is nonnegative with mass $p_T(r)(1-p_T(r))$, and, for every fixed $k \ge 0$,

$$C_{k,T}(r) = p^2 + \int_0^\infty \Omega_d(kt)\,\mathrm{d}\mu_{f,T}(t) + O(T^{-1}).$$

If $s : \mathbb{R}^d \to \{-1,1\}$ is measurable, let $\nu_{s,T}$ be the measure on Fourier radii associated with s_T. It is nonnegative with mass 1 and satisfies

$$C_{k,T}(s) = \int_0^\infty \Omega_d(kt)\,\mathrm{d}\nu_{s,T}(t) + O(T^{-1}).$$

For $T \ge k$, the error in the first formula has absolute value at most $2D_dk/T$, and the error in the second formula has absolute value at most D_dk/T.

Proof. The measure $\mu_{f,T}$ is nonnegative by definition. Lemma 11 and the identity $r^2 = r$ show that its mass is

$$\frac{1}{|B_T|}\int_{B_T}(r-p)^2\,\mathrm{d}x = p - 2p^2 + p^2 = p(1-p).$$

Lemma 12 applied to f_T gives $C_{k,T}(f_T) = \int_0^\infty \Omega_d(kt)\,\mathrm{d}\mu_{f,T}(t) + E_{k,T}$, where $|E_{k,T}| \le D_dk/T$ when $T \ge k$. To express the left side in terms of r, define

$$A_{k,T} = \frac{1}{|B_T|}\int_{\mathbb{S}^{d-1}}\int_{B_T} r(x+k\omega)\,\mathrm{d}x\,\mathrm{d}\sigma_{d-1}(\omega).$$

When $k = 0$, $A_{0,T} = p$ and both identities below are exact, with zero boundary error. Assume $k > 0$ for the remaining discussion. Expanding $(r(x)-p)(r(x+k\omega)-p)$ gives a term $C_{k,T}(r)$. The average of the first factor is $p_T(r) = p$, so the constant terms cancel and

$$C_{k,T}(f_T) = C_{k,T}(r) - pA_{k,T}.$$

For each ω, translation by $k\omega$ changes the domain of integration from B_T to $B_T + k\omega$. Equation (2.2) and $0 \le r \le 1$ therefore give $|A_{k,T} - p| \le D_dk/T$. Hence $C_{k,T}(f_T) = C_{k,T}(r) - p^2 + E'_{k,T}$, where $|E'_{k,T}| \le D_dk/T$. Combining this with the error $E_{k,T}$ gives the stated $2D_dk/T$ bound and proves the first formula.

For s, use the radial measure $\nu_{s,T}$ associated with s_T and apply Lemmas 11 and 12 to s. The mass of this measure is 1 because $s^2 = 1$, and the explicit error bound is D_dk/T. □

The planar expressions are finite sums of one-point terms and products of two values of a coloring. The next proposition averages every such expression at once. Its kernel is obtained by replacing each product at distance r by $J_0(rt)$.

For the next proposition, let $P \subset \mathbb{R}^2$ be finite, with $|p| \le M$ for every $p \in P$, and let $h_1, \ldots, h_s : \mathbb{R}^2 \to [-1,1]$ be measurable. In every sum indexed by $\{p,q\} \subset P$, the pairs are unordered two-element subsets of P, so each pair occurs once. For real coefficients c, $\alpha_{j,p}$, and $\beta_{j,pq} = \beta_{j,qp}$, define

$$\mathcal{L}_{x,\theta} := c + \sum_{j=1}^{s}\sum_{p\in P}\alpha_{j,p}h_j(x+\rho_\theta p) + \sum_{j=1}^{s}\sum_{\{p,q\}\subset P}\beta_{j,pq}h_j(x+\rho_\theta p)h_j(x+\rho_\theta q).$$

Put $K_j(t) = \sum_{\{p,q\}\subset P} \beta_{j,pq} J_0(|p-q|t)$. For $T > 2M$, let A_T be the average of $\mathcal{L}_{x,\theta}$ over $B_T \times [0, 2\pi]$:

$$A_T := \frac{1}{2\pi|B_T|}\int_0^{2\pi}\int_{B_T} \mathcal{L}_{x,\theta}\,\mathrm{d}x\,\mathrm{d}\theta.$$

Here $\nu_{h_j,T}$ is the measure on Fourier radii obtained from $\widehat{\nu}_{h_j,T}$ by mapping ξ to $|\xi|$.

Proposition 15. *With this notation, if $T > 2M$, then*

$$\left|\begin{aligned} &A_T - c - \sum_{j=1}^{s}\left(\sum_{p\in P}\alpha_{j,p}\right) p_T(h_j) \\ &\qquad - \sum_{j=1}^{s}\int_0^\infty K_j(t)\,\mathrm{d}\nu_{h_j,T}(t)\end{aligned}\right| \le \frac{4M}{T}\sum_{j,p}|\alpha_{j,p}| + \frac{12M}{T}\sum_{j,\{p,q\}}|\beta_{j,pq}|.$$

Proof. For each j and $p \in P$, equation (2.3) gives

$$\frac{1}{2\pi|B_T|}\int_0^{2\pi}\int_{B_T} h_j(x+\rho_\theta p)\,\mathrm{d}x\,\mathrm{d}\theta = p_T(h_j) + \varepsilon_{j,p},$$

where $|\varepsilon_{j,p}| \le 4M/T$. Thus the total contribution of the linear terms is

$$\sum_{j=1}^{s}\left(\sum_{p\in P}\alpha_{j,p}\right) p_T(h_j) + E_1.$$

Here $|E_1| \le (4M/T)\sum_{j,p}|\alpha_{j,p}|$. For each j and each unordered pair $\{p,q\}\subset P$, equation (2.4) similarly gives

$$\frac{1}{2\pi|B_T|}\int_0^{2\pi}\int_{B_T} h_j(x+\rho_\theta p)h_j(x+\rho_\theta q)\,\mathrm{d}x\,\mathrm{d}\theta = \int_0^\infty J_0(|p-q|t)\,\mathrm{d}\nu_{h_j,T}(t) + \varepsilon_{j,pq},$$

where $|\varepsilon_{j,pq}| \le 12M/T$. It follows that the total contribution of the quadratic terms is

$$\sum_{j=1}^{s}\sum_{\{p,q\}\subset P}\beta_{j,pq}\int_0^\infty J_0(|p-q|t)\,\mathrm{d}\nu_{h_j,T}(t) + E_2,$$

where $|E_2| \le (12M/T)\sum_{j,\{p,q\}}|\beta_{j,pq}|$. The sums are finite, so they may be interchanged with the integrals. For each j, the resulting integrand is $\sum_{\{p,q\}\subset P}\beta_{j,pq}J_0(|p-q|t) = K_j(t)$. Adding the constant, linear, and quadratic contributions gives the stated formula. Its error is $E_1 + E_2$, the sum of the linear and quadratic truncation errors, and the triangle inequality gives the claimed bound. $\square$

Proposition 16. *Use the notation of Proposition 15. Suppose a finite local argument shows that every allowed coloring of P satisfies $\mathcal{L} \ge c_0$, and that every translated and rotated copy of P in a measurable global coloring avoiding the target configurations is allowed. Put*

$$A_j = \sum_{p\in P}\alpha_{j,p}, \qquad m_{j,T} = \nu_{h_j,T}([0,\infty)),$$

The boundary constant in Proposition 15 is

$$C_{\mathrm{bd}} = 4M\sum_{j,p}|\alpha_{j,p}| + 12M\sum_{j,\{p,q\}}|\beta_{j,pq}|.$$

Assume that there are numbers $\kappa_1, \ldots, \kappa_s$ *and* $\eta > 0$ *such that* $K_j(t) \le \kappa_j$ *for every* j *and* $t \ge 0$*, and that the density and Fourier masses arising from the global coloring satisfy*

$$c + \sum_{j=1}^{s} A_j p_T(h_j) + \sum_{j=1}^{s} \kappa_j m_{j,T} \le c_0 - \eta$$

for every $T > 2M$*. Then no such global coloring exists. More specifically, the contradiction is obtained for any*

$$T > \max\left\{2M, \frac{C_{\mathrm{bd}}}{\eta}\right\}.$$

Proof. The local hypothesis gives $A_T \ge c_0$. Since the measures $\nu_{h_j,T}$ are nonnegative, the kernel bounds give

$$\sum_{j=1}^{s} \int_0^\infty K_j(t)\,\mathrm{d}\nu_{h_j,T}(t) \le \sum_{j=1}^{s} \kappa_j m_{j,T}.$$

Proposition 15 therefore gives $A_T \le c_0 - \eta + C_{\mathrm{bd}}/T < c_0$, a contradiction. □

2.3. **Analytic estimates.** The preceding results reduce the later proofs to pointwise estimates for finite linear combinations of the functions $\Omega_d(rt)$. We record here the elementary bounds used outside bounded intervals. On bounded intervals, the later proofs combine the derivative estimate in Lemma 10 with values checked at finitely many points.

Lemma 17. *The following estimates hold:*

(i) $|J_0'(x)| < 2/3$ *for every* $x \in \mathbb{R}$.
(ii) If $x \ge 2$*, then* $|J_0(x)| \le \sqrt{2/(\pi x)}$.
(iii) If $q \ge 1$ *and* $t \ge 25$*, then* $|J_0(\sqrt{q}\,t)| < 1/(6q^{1/4})$.
(iv) If $q \ge 1$ *and* $t \ge 100$*, then* $|J_0(\sqrt{q}\,t)| < 5/(6\sqrt{t}\,q^{1/4})$.
(v) If $t > 0$*, then* $|\Omega_3(t)| \le 1/t$.
(vi) If $t > 0$*, then* $|\Omega_4(t)| \le 2/t$.
(vii) If $t \ge 10$*, then* $|\Omega_7(t)| \le 30/t^3$.

Proof. The integral representation $J_0(x) = \pi^{-1} \int_0^\pi \cos(x \sin\theta)\,\mathrm{d}\theta$ [26, Eq. 10.9.1] may be differentiated under the integral sign, so $|J_0'(x)| \le 2/\pi < 2/3$.

For (ii), put $\chi = x - \pi/4$. The expansion and signed remainder theorem in [26, Eq. 10.17.3 and Sec. 10.17(iii)] give

$$J_0(x) = \sqrt{\frac{2}{\pi x}}\Big(A(x)\cos\chi + B(x)\sin\chi\Big),$$

where

$$A = 1 - \frac{9}{128x^2} + R_e, \qquad B = \frac{1}{8x} - R_o,$$

and $0 \le R_e \le 11025/(98304x^4)$, $0 \le R_o \le 225/(3072x^3)$. For $x \ge 2$, one has $0 \le A \le 1 - 9/(128x^2) + 11025/(98304x^4)$ and $0 \le B \le 1/(8x)$. Thus it suffices to show that the squares of these two upper bounds sum to at most 1. With $y = x^{-2} \le 1/4$, clearing denominators reduces this to

$$134217728 - 246153216y + 16934400y^2 - 13505625y^3 > 0,$$

which follows by replacing y by $1/4$ in the two negative terms. Cauchy–Schwarz now gives (ii).

Substituting $x = \sqrt{q}\,t$ into (ii) gives $|J_0(\sqrt{q}\,t)| \le q^{-1/4}\sqrt{2/(\pi t)}$. Using $\pi > 3$ gives (iii) and (iv). The formula $\Omega_3(t) = \sin t/t$ gives (v), while the integral representation of J_1 [26, Eq. 10.9.2] gives $|J_1(t)| \le 1$ and hence (vi). Finally, $|\Omega_7(t)| \le 15(t^2+3t+3)/t^5 \le 30/t^3$ for $t \ge 10$. $\square$

For the checks on bounded intervals below, write $u = z^2/4$. If the series for $J_0(z)$ is truncated after the term with index N and $u < (N+2)^2$, then the successive tail terms have ratio at most $u/(N+2)^2$. Thus the omitted tail satisfies

$$\left|\sum_{m=N+1}^{\infty} \frac{(-1)^m u^m}{(m!)^2}\right| \le \frac{u^{N+1}}{((N+1)!)^2}\frac{1}{1-u/(N+2)^2}. \tag{2.5}$$

We will repeatedly use the following consequence of the mean value theorem: if $|K'| \le D$ on an interval and every point of the interval lies within $h/2$ of a checked point where $K \le M$, then $K \le M + Dh/2$ throughout the interval.

At a rational sample point t, the series parameter $u = qt^2/4$ is rational whenever the squared distance q is rational, so the partial sum and the right side of (2.5) are rational. When q is irrational, we enclose it by rational endpoints and propagate the interval through the series with outward rounding. The coefficient sign then selects the endpoint used in an upper or lower kernel bound. The derivative estimates in the corresponding proof extend the sample-point bounds between sample points. For the two planar configurations $W_4(\sqrt{2})$ and P_5, the corresponding finite checks are summarized in Appendix A. That appendix gives the finite sets of colorings and line-graph vertices, exact arithmetic, rational interval bounds, and bounds for the omitted series terms used in those checks.

3. Proof of Theorem 1

3.1. **The finite planar inequality.** Let $e_1, e_2 \in \mathbb{R}^2$ be unit vectors satisfying $e_1 \cdot e_2 = 1/2$. For $i \in \{0,1\}$ and $0 \le j \le 8$, put $v_{ij} = (i-1/2)e_1 + (j-4)e_2$, and set $P = \{v_{ij} : i \in \{0,1\},\ 0 \le j \le 8\}$. We use the label ij for v_{ij}. The formula gives $|v_{ij}| \le \sqrt{73}/2$ for every vertex, which will be used in Section 3.2.

For $i \in \{0,1\}$ and $s \in \{0,1,2\}$, put $P_{i,s} = \{v_{ij} : s \le j \le s+6\}$. These are the six copies of ℓ_7 used below, and they are all the copies of ℓ_7 contained in P: a unit-spaced progression in the triangular lattice has label difference $(\Delta i, \Delta j)$ satisfying $\Delta i^2 + \Delta i \Delta j + \Delta j^2 = 1$, whose six possibilities are $(\pm1,0), (0,\pm1), (1,-1), (-1,1)$. Since $i \in \{0,1\}$, a progression of seven points must have $\Delta i = 0$ and $|\Delta j| = 1$, so it is one of the sets $P_{i,s}$.

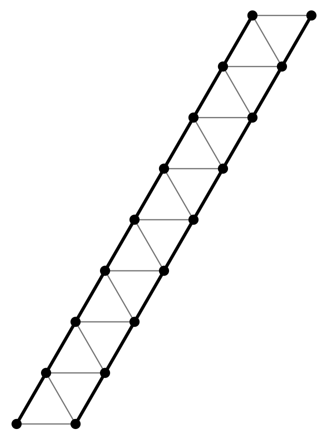

FIGURE 1. The eighteen-point triangular-lattice strip P; all drawn edges have unit length.

For a coloring $\mathrm{Col} : P \to \{R, B\}$, let r_p be the red indicator and put $b_p = 1 - r_p$. Define

$$N_R = \sum_{p \in P} r_p, \qquad N_B = \sum_{p \in P} b_p.$$

For each vertex $p \in P$ and unordered pair $\{p, w\} \subset P$, let c_p and $a_{pw} = a_{wp}$ be the integer coefficients in the local inequality. The coefficients were chosen with a linear program and rounded to integers; Lemma 18 checks the resulting inequality. Define

$$V_R = \sum_{p \in P} c_p r_p, \qquad E_R = \sum_{\{p,w\} \subset P} a_{pw} r_p r_w.$$

The eighteen values c_p and the 153 values a_{pw} are listed in Appendix B, so $\mathcal{L}$ is explicitly defined.

Define

$$\mathcal{L} = -1000 + \frac{500}{9} N_R + \frac{500}{9} N_B + V_R + E_R, \tag{3.1}$$

If the configuration has no red unit edge, then every pair term corresponding to a unit pair vanishes. Also, $N_R + N_B = 18$, so the first three terms in (3.1) are $-1000 + (500/9) \cdot 18 = 0$. Since the remaining coefficients and indicators are integers, $\mathcal{L}$ is integer-valued.

Lemma 18. *If a coloring of P has no red unit edge and none of the six sets $P_{i,s}$ is entirely blue, then $\mathcal{L} \geq 1$.*

Proof. For a subset $R \subseteq P$, let Col_R be the coloring whose red set is R, and write $r_p(R) = \mathbf{1}_R(p)$. Define

$$F(R) = \sum_{p \in P} c_p r_p(R) + \sum_{\{p,q\} \subset P} a_{pq} r_p(R) r_q(R).$$

For Col_R, one has $N_R = |R|$ and $N_B = 18 - |R|$, so the first three terms in (3.1) cancel and $F(R)$ is the value of $\mathcal{L}$ on Col_R.

The unit pairs in the labeling $00, 01, \dots, 08, 10, 11, \dots, 18$ are

$$\begin{aligned} &\{v_{ij}, v_{i,j+1}\} \text{ for } i \in \{0,1\},\ 0 \le j \le 7, \\ &\{v_{0j}, v_{1j}\} \text{ for } 0 \le j \le 8, \\ &\{v_{0j}, v_{1,j-1}\} \text{ for } 1 \le j \le 8. \end{aligned}$$

Let $\mathcal{A}_7$ be the family of subsets $R \subseteq P$ such that no unit pair is contained in R and $R \cap P_{i,s} \neq \varnothing$ for $i \in \{0,1\}$ and $s \in \{0,1,2\}$. The first condition excludes red unit pairs, and the second excludes blue copies of ℓ_7. Thus it suffices to check $F(R) \ge 1$ for $R \in \mathcal{A}_7$.

The finite check over $\mathcal{A}_7$ leaves 751 subsets. Substitution of the integer coefficients from Appendix B gives $F(R) \ge 1$ for every $R \in \mathcal{A}_7$, which proves the lemma. ☐

3.2. **Averaging the local expression.** To compute the average of $\mathcal{L}$, we now group its pair terms according to squared distance. For integer pairs $p = (i,j)$ and $q = (i', j')$, write $Q(p-q) = (i-i')^2 + (i-i')(j-j') + (j-j')^2$.

Lemma 19. *For vertices labelled by $p, q \in \{0,1\} \times \{0,1,\dots,8\}$, one has $|v_p - v_q|^2 = Q(p-q)$.*

Proof. Write $\Delta i = i - i'$ and $\Delta j = j - j'$. Since $|e_1| = |e_2| = 1$ and $e_1 \cdot e_2 = 1/2$, one has $|v_p - v_q|^2 = (\Delta i)^2 + \Delta i \Delta j + (\Delta j)^2 = Q(p-q)$. ☐

Suppose that a measurable coloring $\mathrm{COL} : \mathbb{R}^2 \to \{R, B\}$ contains no red ℓ_2 and no blue ℓ_7. Let r be the red indicator and put $b = 1 - r$. For $x \in \mathbb{R}^2$ and $\theta \in \mathbb{R}$, the coloring induced on P is $\mathrm{Col}_{x,\theta} = (\mathrm{COL}(x + \rho_\theta v))_{v \in P}$. For $T > \sqrt{73}$, set

$$A_T = \frac{1}{2\pi |B_T|} \int_0^{2\pi} \int_{B_T} \mathcal{L}(\mathrm{Col}_{x,\theta}) \, \mathrm{d}x \, \mathrm{d}\theta.$$

Every induced coloring satisfies Lemma 18, so $A_T \ge 1$.

Define

$$\begin{aligned} H_R(t) = 681 &- 489 J_0(t) + 1035 J_0(\sqrt{3}t) - 669 J_0(2t) \\ &+ 600 J_0(\sqrt{7}t) - 700 J_0(3t) + 548 J_0(\sqrt{13}t) \\ &- 355 J_0(4t) + 441 J_0(\sqrt{21}t) - 105 J_0(5t) \\ &+ 339 J_0(\sqrt{31}t) - 114 J_0(6t) - 139 J_0(\sqrt{43}t) \\ &+ 16 J_0(7t) - 90 J_0(\sqrt{57}t), \end{aligned} \tag{3.2}$$

$$H_B(t) = 1000. \tag{3.3}$$

The distance-class data underlying this grouping are recorded in Appendix A.2.

Proposition 20. *For every $T > \sqrt{73}$,*

$$\left| A_T + 1000 - \int_0^\infty H_R(t) \, \mathrm{d}\nu_{r,T}(t) - \int_0^\infty H_B(t) \, \mathrm{d}\nu_{b,T}(t) \right| \le \frac{54734\sqrt{73}}{T}. \tag{3.4}$$

Moreover,

$$\nu_{r,T}([0,\infty)) + \nu_{b,T}([0,\infty)) = 1. \tag{3.5}$$

Proof. The patch has radius $M_0 = \sqrt{73}/2$. From the coefficients in Appendix B, the absolute sums of the linear and quadratic coefficients are 1681 and 8562. Proposition 15 therefore gives the error

$$\frac{4M_0}{T}\,1681 + \frac{12M_0}{T}\,8562 = \frac{54734\sqrt{73}}{T}.$$

The linear coefficient sums are 681 for red and 1000 for blue; the blue part has no quadratic terms. Grouping the red pair coefficients by squared distance gives (3.2), so Proposition 15 gives (3.4). Finally, the two measures have masses $p_T(r)$ and $p_T(b)$, and $r + b = 1$, which gives (3.5). □

3.3. **Bounds for the kernel.** Put $K = H_R - 1000$. The finite interval calculation used below is recorded in Appendix A.2.

Proposition 21. *For every $t \geq 0$, one has $H_R(t) < 1000$.*

Proof. Put $K = H_R - 1000$. Appendix A.2 gives rational upper bounds for K on $[0, 100]$, together with a derivative bound that extends them between the checked points. Hence $K < 0$ on this interval.

For $t \geq 100$, the same appendix gives $\sum_q |A_q| q^{-1/4} < 3600$. Lemma 17 therefore yields

$$H_R(t) \leq 681 + \frac{5}{6\sqrt{t}} \sum_q \frac{|A_q|}{q^{1/4}} < 681 + 300 = 981 < 1000.$$

□

Proof of Theorem 1. Choose $T > 54734\sqrt{73}$. This choice also satisfies $T > \sqrt{73}$, so Lemma 18 and Proposition 20 give the following bound. This is the planar averaging argument of Proposition 16: the local lemma supplies the lower bound, while the Fourier proposition supplies the averaged upper bound.

$$1 \leq A_T \leq -1000 + \int_0^\infty H_R(t)\,\mathrm{d}\nu_{r,T}(t) + \int_0^\infty H_B(t)\,\mathrm{d}\nu_{b,T}(t) + \frac{54734\sqrt{73}}{T}.$$

Proposition 21, (3.3), and (3.5), together with positivity of the two measures, imply $A_T \leq 54734\sqrt{73}/T$. This is less than 1 when $T > 54734\sqrt{73}$, contradicting $A_T \geq 1$. □

4. Proof of Theorem 2

4.1. **A quadratic expression on a nine-point patch.** Let $e_1, e_2 \in \mathbb{R}^2$ be unit vectors with $e_1 \cdot e_2 = 1/2$. Put $v_{ij} = (i-1)e_1 + (j-1)e_2$ for $0 \leq i, j \leq 2$, and let $\Lambda = \{v_{ij} : 0 \leq i, j \leq 2\}$. We label v_{ij} by ij.

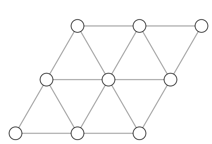

FIGURE 2. The nine-point triangular-lattice configuration Λ.

For integer pairs $p = (i, j)$ and $q = (i', j')$, put $Q(p - q) = (i - i')^2 + (i - i')(j - j') + (j - j')^2$. Then $|v_{ij} - v_{i'j'}|^2 = Q((i, j) - (i', j'))$. The nonzero squared distances in Λ are $1, 3, 4, 7, 12$. The copies of ℓ_3 used below lie in the three unit directions $(1, 0)$, $(0, 1)$, and $(1, -1)$.

Let $\mathcal{G}$ be generated by $\sigma(i, j) = (j, i)$ and $\tau(i, j) = (2 - i, 2 - j)$. It has four elements and preserves the configuration and its distances. Its vertex orbits are

representative	orbit	size
00	$\{00, 22\}$	2
01	$\{01, 10, 12, 21\}$	4
02	$\{02, 20\}$	2
11	$\{11\}$	1.

The action on unordered pairs has thirteen orbits. Let $\mathcal{O}_V$ and $\mathcal{O}_P$ denote the vertex and pair orbits, respectively. For $U \in \mathcal{O}_P$, let $d(U)$ be the common squared distance of the pairs in U.

For a coloring with colors G, R, B, define $g = 1_G$ and $s = 1_R - 1_B$. Thus $g^2 = g$, $s^2 = 1 - g$, and $gs = 0$. For a vertex orbit O and a pair orbit U, put $[g]_O = |O|^{-1} \sum_{v \in O} g(v)$ and

$$[gg]_U = \frac{1}{|U|} \sum_{\{v,w\} \in U} g(v)g(w),$$

$$[ss]_U = \frac{1}{|U|} \sum_{\{v,w\} \in U} s(v)s(w).$$

A red–blue swap fixes g and changes the sign of s. At one vertex, the relations $g^2 = g$, $s^2 = 1 - g$, and $gs = 0$ reduce every quadratic monomial to a linear combination of 1, g, and s; averaging over the swap removes s. For two distinct vertices, the same swap removes the terms containing one factor s, leaving only gg and ss. Averaging over $\mathcal{G}$ then makes each remaining coefficient constant on a vertex or pair orbit.

Define

$$\mathcal{L}(\mathrm{Col}) = -196 + \sum_{O \in \mathcal{O}_V} c_O [g]_O + \sum_{U \in \mathcal{O}_P} \Big(a_U [gg]_U + b_U [ss]_U \Big),$$

where the integer coefficients are the entries in Tables 6 and 7.

By construction, $\mathcal{L}$ is invariant under the symmetry group $\mathcal{G}$ of the configuration: each orbit average is unchanged by the action of $\mathcal{G}$. It is also invariant under interchanging red and blue, since this fixes g, sends s to $-s$, and the expression contains s only through products $s(v)s(w)$.

Lemma 22. *Let $V = \{0, 1, 2\}^2$, and define*

$$\mathcal{E}_1 = \{\{p, q\} \subseteq V : Q(p - q) = 1\},$$
$$\mathcal{I}_3 = \{(p, p + u, p + 2u) : u \in \{(1, 0), (0, 1), (1, -1)\}, p, p + u, p + 2u \in V\}.$$

Let $\mathcal{A}_3$ be the set of colorings $c : V \to \{G, R, B\}$ for which no pair in $\mathcal{E}_1$ has color RR or BB, and no triple in $\mathcal{I}_3$ has color GGG. Then $|\mathcal{A}_3| = 304$, and $4\mathcal{L}(c) \geq 0$ for every $c \in \mathcal{A}_3$, with equality for at least one coloring.

Proof. The set $\mathcal{E}_1$ contains the 16 unit pairs in the configuration, and $\mathcal{I}_3$ contains the 7 copies of ℓ_3 in the three unit directions $(1,0)$, $(0,1)$, and $(1,-1)$. For a coloring satisfying these local restrictions, put $g_p = 1_{\{c(p)=G\}}$ and $s_p = 1_{\{c(p)=R\}} - 1_{\{c(p)=B\}}$. Then

$$\begin{aligned} F(c) = 4\mathcal{L}(c) = & -784 + \sum_{O\in\mathcal{O}_V} \frac{4c_O}{|O|} \sum_{p\in O} g_p \\ & + \sum_{U\in\mathcal{O}_P} \frac{4}{|U|}\left(a_U \sum_{\{p,q\}\in U} g_p g_q + b_U \sum_{\{p,q\}\in U} s_p s_q\right). \end{aligned}$$

The orbit sizes are 1, 2, or 4, so $4/|O|$ and $4/|U|$ are integers; also $g_p, s_p \in \{-1,0,1\}$. Thus $4\mathcal{L}(c) = F(c)$ is integer-valued. There are 304 colorings satisfying the local restrictions, and substitution gives $F(c) \geq 0$ for each of them. □

Lemma 23. *If a coloring of Λ contains no red ℓ_2, no blue ℓ_2, and no green ℓ_3, then $\mathcal{L} \geq 0$.*

Proof. The condition that no red or blue unit pair occurs is the condition that no pair in $\mathcal{E}_1$ has color RR or BB, because $Q(p-q) = 1$ lists every unit pair of Λ. Likewise, the stated definition of $\mathcal{I}_3$ lists every three-point unit-spaced collinear copy of ℓ_3 in Λ. Hence the coloring belongs to $\mathcal{A}_3$, and the preceding lemma gives $4\mathcal{L} \geq 0$. □

4.2. **Averaging the local expression.** Suppose that a measurable coloring of $\mathbb{R}^2$ contains none of the three configurations in Theorem 2, and apply the same definitions of g and s pointwise. For $x \in \mathbb{R}^2$ and $\theta \in \mathbb{R}$, let $\mathrm{Col}_{x,\theta}$ be the coloring induced on $x + \rho_\theta\Lambda$, and set

$$A_T = \frac{1}{2\pi|B_T|}\int_0^{2\pi}\int_{B_T} \mathcal{L}(\mathrm{Col}_{x,\theta})\,\mathrm{d}x\,\mathrm{d}\theta.$$

Lemma 23 gives $A_T \geq 0$.

Grouping the coefficients by squared distance gives

$$\begin{aligned} H_g(t) = & -603 - 1050J_0(t) + 1610J_0(\sqrt{3}t) - 1152J_0(2t) \\ & + 1000J_0(\sqrt{7}t) + 375J_0(\sqrt{12}t), \end{aligned} \tag{4.1}$$

$$\begin{aligned} H_s(t) = & -442J_0(t) + 138J_0(\sqrt{3}t) - 12J_0(2t) \\ & + 300J_0(\sqrt{7}t) + 200J_0(\sqrt{12}t). \end{aligned} \tag{4.2}$$

Proposition 24. *For every $T > 2\sqrt{3}$,*

$$\left|A_T + 196 - \int_0^\infty H_g(t)\,\mathrm{d}\nu_{g,T}(t) - \int_0^\infty H_s(t)\,\mathrm{d}\nu_{s,T}(t)\right| \leq \frac{134272\sqrt{3}}{T}. \tag{4.3}$$

Moreover,

$$\nu_{g,T}([0,\infty)) + \nu_{s,T}([0,\infty)) = 1. \tag{4.4}$$

Proof. Every point of Λ has norm at most $\sqrt{3}$. The absolute sums of the linear and quadratic coefficients are 2599 and 10323, respectively, so Proposition 15 gives the error

$$\frac{4\sqrt{3}}{T}2599 + \frac{12\sqrt{3}}{T}10323 = \frac{134272\sqrt{3}}{T}.$$

The vertex coefficients sum to -603, and grouping the pair coefficients by distance gives (4.1)–(4.2); hence (4.3). Pointwise $g + s^2 = 1$, so Lemma 11 gives (4.4). $\square$

4.3. **Bounds for the kernels.**

Proposition 25. *For every $t \geq 0$, one has $H_g(t) < 193$ and $H_s(t) < 193$.*

Proof. On $[0, 25]$, Appendix A gives $H_g(t_j) < 180$ and $H_s(t_j) < 46019/250$ at $t_j = j/400$. Lemma 17 and the chain rule give $\|H_g'\|_\infty < 30452/3$ and $\|H_s'\|_\infty < 4415/2$ on this interval. The mean value theorem then gives

$$H_g(t) < 180 + \frac{30452/3}{800} < 193, \qquad H_s(t) < \frac{46019}{250} + \frac{4415/2}{800} < 193.$$

For $t \geq 25$, Lemma 17 and (4.1)–(4.2), using $3^{-1/4} < 10/13$, $4^{-1/4} < 5/7$, $7^{-1/4} < 5/8$, and $12^{-1/4} < 5/9$, give $H_g(t) < 55$ and $H_s(t) < 143$. $\square$

Proof of Theorem 2. Choose $T = 100000$. The measures $\nu_{g,T}$ and $\nu_{s,T}$ are nonnegative, so Propositions 24 and 25, together with (4.4), give the following chain. This is another application of Proposition 16, with the nine-point local inequality providing the lower bound and the two kernel estimates providing the upper bound.

$$\begin{aligned}
0 &\leq A_T \\
&\leq -196 + \int_0^\infty H_g \, \mathrm{d}\nu_{g,T} + \int_0^\infty H_s \, \mathrm{d}\nu_{s,T} + \frac{134272\sqrt{3}}{T} \\
&\leq -196 + 193\Big(\nu_{g,T}([0,\infty)) + \nu_{s,T}([0,\infty))\Big) + \frac{134272\sqrt{3}}{T} \\
&= -3 + \frac{134272\sqrt{3}}{T} \\
&< 0.
\end{aligned}$$

Here $134272\sqrt{3} < 300000$, so the final inequality holds for the chosen T. This contradiction proves Theorem 2. $\square$

5. Proofs of Theorems 3–6

5.1. **Line inequalities and averaging.** The four proofs begin with the same finite directed-graph lemma.

Lemma 26. *Let $G = (V, E)$ be a finite directed graph, assign a real weight $w : E \to \mathbb{R}$ to each edge, and let $\phi : V \to \mathbb{R}$ satisfy*

$$w(u, v) + \phi(u) - \phi(v) \geq 0$$

on every edge, then every directed path $v_0, \ldots, v_N$ satisfies

$$\sum_{j=0}^{N-1} w(v_j, v_{j+1}) \geq \phi(v_N) - \phi(v_0).$$

Proof. For a directed path $v_0, \dots, v_N$, summing the edge inequalities gives

$$\begin{aligned} 0 &\le \sum_{j=0}^{N-1} \Big(w(v_j, v_{j+1}) + \phi(v_j) - \phi(v_{j+1}) \Big) \\ &= \sum_{j=0}^{N-1} w(v_j, v_{j+1}) + \sum_{j=0}^{N-1} \Big(\phi(v_j) - \phi(v_{j+1}) \Big) \\ &= \sum_{j=0}^{N-1} w(v_j, v_{j+1}) + \phi(v_0) - \phi(v_N). \end{aligned}$$

Rearranging gives the stated inequality. □

The function ϕ records the contribution of the current local pattern. When the local inequality is summed along a line, all intermediate values cancel and only the two endpoint values remain. The averaging argument below is the same cancellation with a boundary error.

For a red–blue coloring, let $r = 1_R$ and $s = 1_R - 1_B$. Here $\omega \in \mathbb{S}^{d-1}$ is a unit direction vector, so $x + \mathbb{R}\omega$ is the line through x in direction ω. On this oriented line, write $r_j = r(x + j\omega)$ and $s_j = s(x + j\omega)$. If there is no red ℓ_a and no blue ℓ_b, then the binary sequence $(r_j)_{j\in\mathbb{Z}}$ contains neither the consecutive string 1^a nor the consecutive string 0^b. In the $\{-1, 1\}$-encoding, the absence of a monochromatic ℓ_4 says that no four consecutive signs are equal.

The graph vertices below are represented by binary sequences. Thus, in the (ℓ_4, ℓ_4) case, put

$$\epsilon_j = r_j = \frac{s_j + 1}{2} \in \{0, 1\}.$$

The sequence $\epsilon_0 \cdots \epsilon_3$ avoids the forbidden consecutive patterns unless it is 0000 or 1111, while the signed variables in W_{44} are obtained from the same sequence by $s_j = 2\epsilon_j - 1$. In the other three cases the entries are already the binary values used by r_j.

Let $Q = \{34, 35, 36, 44\}$. For $q \in Q$, define F_q and m_q by

q	F_q	m_q
34	$\{111, 0000\}$	3
35	$\{111, 00000\}$	6
36	$\{111, 000000\}$	6
44	$\{1111, 0000\}$	4

A finite binary sequence avoids F_q when it contains no member of F_q consecutively. Define the vertex and edge sets by

$$\mathcal{V}_q = \{u \in \{0,1\}^{m_q} : u \text{ avoids } F_q\},$$

and

$$\mathcal{E}_q = \left\{ (u, v) \in \mathcal{V}_q^2 : \begin{array}{l} u_1 \cdots u_{m_q-1} = v_0 \cdots v_{m_q-2}, \\ u_0 \cdots u_{m_q-1} v_{m_q-1} \text{ avoids } F_q \end{array} \right\}.$$

Thus forbidden consecutive patterns are excluded both from the vertex set and from the length-$(m_q + 1)$ sequence associated with an edge. The direction $u \to v$ moves one position to the left and appends the next color, so it records adding one point along the oriented line.

The sequence length is chosen so that the forbidden patterns and every entry in the local expression are determined by one edge. A coloring of an oriented line therefore gives a directed path in the corresponding graph. The resulting numbers of vertices and edges are recorded in Table 1 in the appendix. For an allowed edge, define

$$\begin{aligned}
W_{34} &= 4r_0 - 1 - 3r_0r_1 - 2r_0r_2, \\
W_{35} &= -6 + 28r_0 - 20r_0r_1 - 14r_0r_2 - 3r_0r_3 - 4r_0r_4 + 2r_0r_5 + 2r_0r_6, \\
W_{36} &= -2 + 11r_0 - 9r_0r_1 - 5r_0r_2 - 2r_0r_4 - r_0r_5 + r_0r_6, \\
W_{44} &= -1 - 6s_0s_1 - 4s_0s_2 - 2s_0s_3 + s_0s_4.
\end{aligned}$$

Here r_j and s_j are the colors at the successive points of the length- (m_q+1) sequence associated with the edge. The expressions are chosen so that their averages over all translated and oriented lines involve only the correlations listed below. The four expressions and accompanying vertex potentials are the integer data recorded in Appendix B. The four potentials are listed there explicitly for every vertex in the corresponding set $\mathcal{V}_q$. Only these listed values are used below.

Proposition 27. *For each $q \in Q$, let $\phi_q : \mathcal{V}_q \to \mathbb{Z}$ be the potential listed in Appendix B. Every allowed edge $(u,v) \in \mathcal{E}_q$ satisfies*

$$W_q(u,v) + \phi_q(u) - \phi_q(v) \geq 0.$$

In the four cases, this is

$$\begin{aligned}
&W_{34} + \phi_{34}(u) - \phi_{34}(v) \geq 0 && ((u,v) \in \mathcal{E}_{34}), \\
&W_{35} + \phi_{35}(u) - \phi_{35}(v) \geq 0 && ((u,v) \in \mathcal{E}_{35}), \\
&W_{36} + \phi_{36}(u) - \phi_{36}(v) \geq 0 && ((u,v) \in \mathcal{E}_{36}), \\
&W_{44} + \phi_{44}(u) - \phi_{44}(v) \geq 0 && ((u,v) \in \mathcal{E}_{44}).
\end{aligned}$$

Proof. For each q, set

$$\sigma_q(u,v) = W_q(u,v) + \phi_q(u) - \phi_q(v).$$

For example, in the (ℓ_3, ℓ_4) graph the edge $000 \to 001$ is associated with the sequence 0001, so

$$W_{34}(0001) = -1, \sigma_{34}(000, 001) = -1 + \phi_{34}(000) - \phi_{34}(001) = -1 + 0 - (-1) = 0.$$

Substituting the integer data from Appendix B gives $\sigma_q(u,v) \geq 0$ for every allowed edge in each of the four graphs. $\square$

Define

$$\begin{aligned}
L_{34,T} &= 4p_T(r) - 1 - 3C_{1,T}(r) - 2C_{2,T}(r),\\
L_{35,T} &= -6 + 28p_T(r) - 20C_{1,T}(r) - 14C_{2,T}(r) - 3C_{3,T}(r)\\
&\quad - 4C_{4,T}(r) + 2C_{5,T}(r) + 2C_{6,T}(r),\\
L_{36,T} &= -2 + 11p_T(r) - 9C_{1,T}(r) - 5C_{2,T}(r) - 2C_{4,T}(r) - C_{5,T}(r) + C_{6,T}(r),\\
L_{44,T} &= -1 - 6C_{1,T}(s) - 4C_{2,T}(s) - 2C_{3,T}(s) + C_{4,T}(s).
\end{aligned}$$

Proposition 28. *For each $q \in Q$, put $M_q = \max_{u\in\mathcal{V}_q} |\phi_q(u)|$. Extend the potential from the finite vertex set to all binary sequences of length m_q by*

$$\bar{\phi}_q(z) = \begin{cases} \phi_q(z), & z \in \mathcal{V}_q,\\ 0, & z \notin \mathcal{V}_q, \end{cases}$$

where $z \in \{0,1\}^{m_q}$. and then to $\mathbb{R}^{m_q}$ by

$$\Phi_q(y_0, \dots, y_{m_q-1}) = \bar{\phi}_q\Big(1_{\{y_0>1/2\}}, \dots, 1_{\{y_{m_q-1}>1/2\}}\Big).$$

Thus Φ_q is bounded and measurable on $\mathbb{R}^{m_q}$, with $|\Phi_q| \le M_q$; in particular it satisfies the boundedness hypothesis of Lemma 12 on the relevant cube. If the corresponding two monochromatic lines are absent, then, for $T \ge 1$,

$$L_{q,T} \ge -\frac{M_q D_{d_q}}{T}.$$

Proof. Fix q and (x, ω). In all four cases let $z_j = r(x + j\omega)$; in the (ℓ_4, ℓ_4) case this is the binary sequence $z_j = \epsilon_j$, and the signed variables in W_{44} are recovered from $s_j = 2z_j - 1$. The avoidance assumption implies that every length-m_q sequence encountered along the line belongs to $\mathcal{V}_q$, and that every length-$(m_q + 1)$ sequence associated with an edge contains no forbidden pattern. Hence the successive vertices form a directed path in the graph. Apply Proposition 27 to the edge corresponding to the length-$(m_q + 1)$ sequence beginning at x, and average this inequality over $B_T \times \mathbb{S}^{d_q-1}$.

The normalized averages of r_0, $r_0 r_k$, and $s_0 s_k$ are, by definition, $p_T(r)$, $C_{k,T}(r)$, and $C_{k,T}(s)$. The remaining two terms are the averages of

$$\Phi_q\Big(z_0(x,\omega), \dots, z_{m_q-1}(x,\omega)\Big) - \Phi_q\Big(z_1(x,\omega), \dots, z_{m_q}(x,\omega)\Big).$$

The shift by one point along the oriented line is the source of this boundary term. The second part of Lemma 12, applied to the bounded extension Φ_q, bounds its absolute value by $M_q D_{d_q}/T$. Removing it leaves the stated lower bound. □

For the next proposition, fix a finite nonempty set K of positive integers, real numbers a, b, and real coefficients $(c_k)_{k\in K}$. Let $r = 1_R$ be a measurable red indicator, write $p = p_T(r)$ and $f_T = r - p_T(r)$, and set

$$S := \sum_{k\in K} c_k,$$

$$H(t) := \sum_{k\in K} c_k \Omega_d(kt).$$

Define

$$L_{r,T} := a + bp + \sum_{k\in K} c_k C_{k,T}(r).$$

Let $\mu_{f,T}$ be the centered-indicator measure associated with f_T in Lemma 14. For a signed coloring $s = 1_R - 1_B$, define

$$L_{s,T} := a + \sum_{k\in K} c_k C_{k,T}(s)$$

and let $\nu_{s,T}$ be the measure associated with s_T from the same lemma. Both measures are nonnegative, with masses $p(1-p)$ and 1, respectively.

Proposition 29. *For $T \geq \max K$, there are errors $E_{r,T}$ and $E_{s,T}$ such that*

$$L_{r,T} = a + bp + Sp^2 + \int_0^\infty H(t)\,\mathrm{d}\mu_{f,T}(t) + E_{r,T}, \quad |E_{r,T}| \leq \frac{2D_d}{T}\sum_{k\in K}|c_k|k,$$

$$L_{s,T} = a + \int_0^\infty H(t)\,\mathrm{d}\nu_{s,T}(t) + E_{s,T}, \qquad |E_{s,T}| \leq \frac{D_d}{T}\sum_{k\in K}|c_k|k.$$

Proof. By Lemma 14, for each $k \in K$ there is an error $E_k(T)$ such that, for $T \geq \max K$,

$$C_{k,T}(r) = p^2 + \int_0^\infty \Omega_d(kt)\,\mathrm{d}\mu_{f,T}(t) + E_k(T),$$
$$|E_k(T)| \leq \frac{2D_d k}{T}.$$

Multiplying by c_k and summing over K, using the definitions of $L_{r,T}$, S, and H, gives

$$L_{r,T} = a + bp + Sp^2 + \int_0^\infty H(t)\,\mathrm{d}\mu_{f,T}(t) + \sum_{k\in K} c_k E_k(T).$$

Set $E_{r,T} = \sum_{k\in K} c_k E_k(T)$. The triangle inequality gives

$$|E_{r,T}| \leq \frac{2D_d}{T}\sum_{k\in K}|c_k|k.$$

If r is replaced by $s = 1_R - 1_B$, the second formula in Lemma 14 gives, for each $k \in K$,

$$C_{k,T}(s) = \int_0^\infty \Omega_d(kt)\,\mathrm{d}\nu_{s,T}(t) + \widetilde{E}_k(T),$$
$$|\widetilde{E}_k(T)| \leq \frac{D_d k}{T},$$

and summing after multiplication by c_k yields

$$L_{s,T} = a + \int_0^\infty H(t)\,\mathrm{d}\nu_{s,T}(t) + \sum_{k\in K} c_k \widetilde{E}_k(T),$$

where $E_{s,T} = \sum_{k\in K} c_k \widetilde{E}_k(T)$. The triangle inequality gives the stated bound. ☐

Proposition 30. *With the notation of Proposition 29, suppose a finite directed graph has vertices u, edges $u \to v$, and a function ϕ on its vertices. Assume that the edge inequalities have the form $W(u,v) + \phi(u) - \phi(v) \geq 0$, so that summing along a line gives, for every coloring avoiding the target configurations, one of the bounds $L_{r,T} \geq -\frac{\kappa_{\mathrm{pot}}}{T}$*

or $L_{s,T} \geq -\frac{\kappa_{\mathrm{pot}}}{T}$ *for some* $\kappa_{\mathrm{pot}} \geq 0$*. Let* $B \in \mathbb{R}$ *satisfy* $H(t) \leq B$ *for all* $t \geq 0$*. In the red-indicator case, assume that*

$$a + bp + Sp^2 + Bp(1-p) \leq -\eta \qquad (0 \leq p \leq 1)$$

for some $\eta > 0$*. In the signed-function case, assume instead that* $a + B \leq -\eta$*. Then the corresponding measurable coloring cannot exist. Define the averaging-error constant*

$$\kappa_{\mathrm{avg}} = \begin{cases} 2D_d \sum_{k \in K} |c_k| k, & \textit{in the red-indicator case,} \\ D_d \sum_{k \in K} |c_k| k, & \textit{in the signed-function case.} \end{cases}$$

The contradiction follows for

$$T > \max\left\{\max K, \frac{\kappa_{\mathrm{pot}} + \kappa_{\mathrm{avg}}}{\eta}\right\}.$$

Proof. In the red-indicator case, Proposition 29, the positivity of $\mu_{f,T}$, and its mass $p(1-p)$ give

$$L_{r,T} \leq a + bp + Sp^2 + Bp(1-p) + \frac{\kappa_{\mathrm{avg}}}{T} \leq -\eta + \frac{\kappa_{\mathrm{avg}}}{T}.$$

The signed-function case is the same calculation with the mass-one measure $\nu_{s,T}$:

$$L_{s,T} \leq a + B + \frac{\kappa_{\mathrm{avg}}}{T} \leq -\eta + \frac{\kappa_{\mathrm{avg}}}{T}.$$

For the stated range of T, either upper bound is smaller than the lower bound supplied by the directed-graph argument. □

For the four coefficient vectors, put

$$\begin{aligned} H_{34}(t) &= -3\Omega_3(t) - 2\Omega_3(2t), \\ H_{35}(t) &= -20\Omega_4(t) - 14\Omega_4(2t) - 3\Omega_4(3t) - 4\Omega_4(4t) + 2\Omega_4(5t) + 2\Omega_4(6t), \\ H_{36}(t) &= -9\Omega_7(t) - 5\Omega_7(2t) - 2\Omega_7(4t) - \Omega_7(5t) + \Omega_7(6t), \\ H_{44}(t) &= -6\Omega_4(t) - 4\Omega_4(2t) - 2\Omega_4(3t) + \Omega_4(4t). \end{aligned}$$

Proposition 31. *For every* $t \geq 0$*,*

$$H_{34}(t) < \frac{7}{10}, \qquad H_{35}(t) < \frac{59}{20},$$
$$H_{36}(t) < \frac{2}{5}, \qquad H_{44}(t) < \frac{9}{10}.$$

Proof. Table 4 gives the checked values, spacings, and derivative bounds on $[0,6]$, $[0,25]$, $[0,10]$, and $[0,25]$, respectively. The mean value theorem gives

$$H_{34}(t) < \frac{69}{100} + \frac{7}{2}\frac{1}{10000} < \frac{7}{10}, \qquad H_{35}(t) < \frac{1469}{500} + \frac{95}{2}\frac{1}{4000} < \frac{59}{20},$$
$$H_{36}(t) < \frac{399}{1000} + \frac{95}{8}\frac{1}{20000} < \frac{2}{5}, \qquad H_{44}(t) < \frac{887}{1000} + 12\frac{1}{5000} < \frac{9}{10}.$$

On the complementary ranges, Lemma 17 applied termwise gives

$$
\begin{aligned}
H_{34}(t) &\le 4/t \le 2/3 && (t \ge 6),\\
H_{35}(t) &\le \frac{2}{t}\left(20 + \frac{14}{2} + \frac{3}{3} + \frac{4}{4} + \frac{2}{5} + \frac{2}{6}\right) < \frac{59}{20} && (t \ge 25),\\
H_{36}(t) &\le \frac{30}{t^3}\left(9 + \frac{5}{2^3} + \frac{2}{4^3} + \frac{1}{5^3} + \frac{1}{6^3}\right) < \frac{2}{5} && (t \ge 10),\\
H_{44}(t) &\le \frac{2}{t}\left(6 + \frac{4}{2} + \frac{2}{3} + \frac{1}{4}\right) < \frac{9}{10} && (t \ge 25).
\end{aligned}
$$

□

For the quantitative estimates below, the integer potentials in Proposition 27 have the bounds on their absolute values in the M_q column of the following table. The last two columns record the boundary constants supplied by Propositions 28 and 29, respectively.

case	D_{d_q}	M_q	$\sum_k \lvert c_{q,k}\rvert k$	κ_q^{pot}	κ_q^{avg}
34	24	3	7	72	336
35	64	30	95	1920	12160
36	896	13	38	11648	68096
44	64	14	24	896	1536

Here κ_q^{pot} and κ_q^{avg} are the constants from the potential argument and the averaging estimate, respectively. We have $\kappa_q^{\mathrm{pot}} = M_q D_{d_q}$; for the first three rows $\kappa_q^{\mathrm{avg}} = 2D_{d_q}\sum_k |c_{q,k}|k$, while for the last row the factor 2 is absent because the coloring is encoded by s.

To make the last step explicit, write $p = p_T(r)$. In the first three cases, Proposition 29 and positivity of $\mu_{f,T}$ allow the integral of H_{ij} to be replaced by its upper bound times $p(1-p)$. The sums of the correlation coefficients are -5, -37, and -16, respectively. Substitution of the bounds from Proposition 31 and completion of the square give

$$L_{34,T} \le -\frac{57}{10}\left(p_T - \frac{47}{114}\right)^2 - \frac{71}{2280} + \frac{336}{T}, \tag{5.1}$$

$$L_{35,T} \le -\frac{799}{20}\left(p_T - \frac{619}{1598}\right)^2 - \frac{359}{63920} + \frac{12160}{T}, \tag{5.2}$$

$$L_{36,T} \le -\frac{82}{5}\left(p_T - \frac{57}{164}\right)^2 - \frac{31}{1640} + \frac{68096}{T}, \tag{5.3}$$

$$L_{44,T} \le -\frac{1}{10} + \frac{1536}{T}. \tag{5.4}$$

For the last line, the measure associated with s has mass 1, so $L_{44,T} \le -1 + 9/10 + 1536/T$.

The next four proofs apply Proposition 30. The edge inequalities give the lower bounds, while (5.1)–(5.4) give the corresponding Fourier upper bounds.

5.2. **Proof of Theorem 3.**

Proof. Assume for contradiction that a measurable red–blue coloring of $\mathbb{E}^3$ contains no red ℓ_3 and no blue ℓ_4. The lower and upper bounds are

$$-\frac{72}{T} \le L_{34,T} \le -\frac{71}{2280} + \frac{336}{T}.$$

They would force

$$T \le \frac{(72+336)\cdot 2280}{71} = \frac{930240}{71},$$

contradicting a choice of T above this threshold. This proves Theorem 3. ☐

5.3. Proof of Theorem 4.

Proof. Assume for contradiction that a measurable red–blue coloring of $\mathbb{E}^4$ contains no red ℓ_3 and no blue ℓ_5. The lower and upper bounds are

$$-\frac{1920}{T} \le L_{35,T} \le -\frac{359}{63920} + \frac{12160}{T}.$$

They would force

$$T \le \frac{(1920+12160)\cdot 63920}{359} = \frac{899993600}{359},$$

contradicting a choice of T above this threshold. This proves Theorem 4. ☐

5.4. Proof of Theorem 5.

Proof. Assume for contradiction that a measurable red–blue coloring of $\mathbb{E}^7$ contains no red ℓ_3 and no blue ℓ_6. The lower and upper bounds are

$$-\frac{11648}{T} \le L_{36,T} \le -\frac{31}{1640} + \frac{68096}{T}.$$

They would force

$$T \le \frac{(11648+68096)\cdot 1640}{31} = \frac{130780160}{31},$$

contradicting a choice of T above this threshold. This proves Theorem 5. ☐

5.5. Proof of Theorem 6.

Proof. Assume for contradiction that a measurable red–blue coloring of $\mathbb{E}^4$ contains no red ℓ_4 and no blue ℓ_4. The lower and upper bounds are

$$-\frac{896}{T} \le L_{44,T} \le -\frac{1}{10} + \frac{1536}{T}.$$

They would force

$$T \le (896+1536)\cdot 10 = 24320,$$

contradicting a choice of T above this threshold. This proves Theorem 6. ☐

The following two planar proofs use Proposition 16. In each case the finite local lemma gives the lower bound for the averaged expression, and the kernel estimate gives the upper bound.

6. Proof of Theorem 7

The finite patches used in the two planar polygon arguments are shown in Figure 3. Solid and dashed polygons indicate the two copies of the configuration; the labels agree with those used in the proofs.

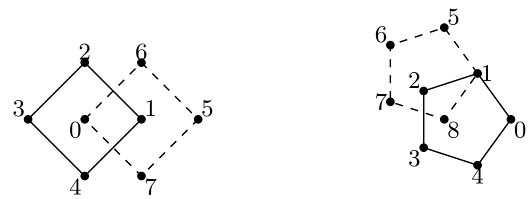

(a) $W_4(\sqrt{2})$ (b) P_5

Figure 3. The finite planar patches used for $W_4(\sqrt{2})$ and P_5.

6.1. **The finite square–center inequality.** Let

$$v_0 = (0,0), \quad v_1 = (1,0), \quad v_2 = (0,1), \quad v_3 = (-1,0),$$
$$v_4 = (0,-1), \quad v_5 = (2,0), \quad v_6 = (1,1), \quad v_7 = (1,-1).$$

The two copies of $W_4(\sqrt{2})$ have index sets $B_0 = \{0,1,2,3,4\}$ and $B_1 = \{1,5,6,0,7\}$. Within this eight-point configuration these are the only copies of $W_4(\sqrt{2})$. Since $x_i = 1$ denotes red, a blue copy is therefore the vertex set B_j on which every x_i is zero. Thus, in the presence of the no-red-unit-pair condition, avoiding a blue $W_4(\sqrt{2})$ is equivalent to requiring that each of B_0 and B_1 contain a red point. The unit-distance pairs among these points are $\mathcal{E}_4 = \{01, 02, 03, 04, 15, 16, 17, 26, 47\}$, where ij denotes the unordered pair $\{i,j\}$.

Put $a = 1/1000$. For $x \in \{0,1\}^8$, define

$$\begin{aligned}
\mathcal{F}_{W_4(\sqrt{2})}(x) = 1 - a &+ a(x_0 + x_1 + x_2 + x_3 + x_5 + x_6) - x_4 - x_7 \\
&- x_0x_1 - x_0x_2 - x_0x_3 - x_0x_4 - ax_0x_5 - ax_0x_6 + x_0x_7 \\
&- ax_1x_2 - ax_1x_3 + x_1x_4 - x_1x_5 - x_1x_6 + ax_1x_7 \\
&- ax_2x_5 + x_2x_6 + x_2x_7 - ax_3x_5 - ax_3x_6 + x_3x_7 \\
&+ x_4x_5 + x_4x_6 + x_4x_7.
\end{aligned}$$

Lemma 32. *Suppose that $x_ix_j = 0$ for every $ij \in \mathcal{E}_4$ and that each of B_0 and B_1 contains an index i with $x_i = 1$. Then $\mathcal{F}_{W_4(\sqrt{2})}(x) \geq 1$.*

Proof. The finite set of binary colorings satisfying the local restrictions is

$$\mathcal{A} = \left\{ x \in \{0,1\}^8 : \begin{array}{c} x_ix_j = 0 \text{ for every } ij \in \mathcal{E}_4, \\ \sum_{i \in B_0} x_i \geq 1 \text{ and } \sum_{i \in B_1} x_i \geq 1 \end{array} \right\}.$$

Enumerating the 2^8 binary colorings gives $|\mathcal{A}| = 37$. Evaluating the integer numerator $1000\mathcal{F}_{W_4(\sqrt{2})}(x)$ on this set gives the values 1000 for 33 colorings, 2000 for two colorings, and 2001 for two colorings. Hence the corresponding values of $\mathcal{F}_{W_4(\sqrt{2})}$ are 1, 2, and 2001/1000. Hence $\mathcal{F}_{W_4(\sqrt{2})}(x) \geq 1$ for every such vector. $\square$

6.2. **The averaged kernel.** The squared distances and the corresponding sums of the quadratic coefficients are

$\lvert v_i - v_j\rvert^2$	1	2	4	5	9
$\sum \beta_{ij}$	$a-4$	$2-2a$	$-2a$	$4-2a$	$-a.$

Thus the radial kernel is

$$K_4(t) = (a-4)J_0(t) + (2-2a)J_0(\sqrt{2}t) - 2aJ_0(2t) + (4-2a)J_0(\sqrt{5}t) - aJ_0(3t).$$

Proposition 33. *For every $t \geq 0$,*

$$K_4(t) \leq 2 - 6a = \frac{997}{500}.$$

Proof. At $t = 0$ equality holds. For $0 < t \leq 1/10$, write

$$(c_1, c_2, c_4, c_5, c_9) = (a-4, 2-2a, -2a, 4-2a, -a).$$

The constant term is

$$\sum_q c_q = 2 - 6a,$$

and the coefficient of t^2 in $(2-6a) - K_4(t)$ is

$$\frac{1}{4}\sum_q qc_q = \frac{1}{4}\Big((a-4) + 2(2-2a) + 4(-2a) + 5(4-2a) + 9(-a)\Big) = \frac{1997}{400}.$$

Using

$$J_0(\sqrt{q}\,t) = \sum_{m=0}^{\infty} \frac{(-1)^m q^m t^{2m}}{4^m (m!)^2},$$

the Bessel series gives

$$(2-6a) - K_4(t) = \frac{1997}{400}t^2 + E_4(t), \qquad E_4(t) = -\sum_q c_q \sum_{m=2}^{\infty} \frac{(-1)^m q^m t^{2m}}{4^m (m!)^2}.$$

Since $qt^2/4 \leq 9/400$ and, for $m \geq 2$, successive absolute terms have ratio at most $1/400$,

$$\begin{aligned}
\frac{|E_4(t)|}{t^2} &\leq \frac{t^2}{64}\left(\sum_q |c_q| q^2\right)\frac{400}{399} \\
&= \frac{t^2}{64}\Big((4-a) + 4(2-2a) + 16(2a) + 25(4-2a) + 81a\Big)\frac{400}{399} \\
&\leq \frac{56027}{500 \cdot 6400} \cdot \frac{400}{399} \\
&< \frac{1997}{400}.
\end{aligned}$$

Thus $K_4(t) < K_4(0)$ on $(0, 1/10]$. On $[1/10, 12]$, the rational interval calculation in Appendix A, together with the derivative bound $|K_4'| < 16$, gives $K_4(t) < 1991/1000 < 997/500$.

For $t \geq 12$, Lemma 17 gives

$$|K_4(t)| \leq \sqrt{\frac{2}{\pi t}} \sum_{q \in \{1,2,4,5,9\}} \frac{|c_q|}{q^{1/4}}, \qquad (c_1, c_2, c_4, c_5, c_9) = (a-4, 2-2a, -2a, 4-2a, -a).$$

The lower bounds $2^{1/4} > 19/16$, $4^{1/4} > 7/5$, $5^{1/4} > 149/100$, and $9^{1/4} > 17/10$ give the sum on the right as less than $42/5$. Since $\pi > 3$ and $\sqrt{18} > 211/50$,

$$|K_4(t)| < \frac{42/5}{\sqrt{18}} < \frac{420}{211} < \frac{997}{500}.$$

□

Proof of Theorem 7. Assume that a measurable coloring has no red unit pair and no blue copy of $W_4(\sqrt{2})$. Let r be the red indicator, put $p = p_T(r)$, and set $f_T = r - p_T(r)$. The local lemma gives $A_T \geq 1$. Expanding $\mathcal{F}_{W_4(\sqrt{2})}(p + f_T)$ and applying Proposition 15 gives

$$A_T = 1 - a + (6a-2)p + (2-6a)p^2 + \int_0^\infty K_4(t)\,\mathrm{d}\mu_{f,T}(t) + E_T,$$

where $\mu_{f,T}$ has mass $p(1-p)$. Here $\sum_i |\alpha_i| = 1003/500$ and $\sum_{i<j} |\beta_{ij}| = 1751/125$. Since the points have norm at most 2, centering changes the linear coefficient sum by at most $2\sum_{i<j} |\beta_{ij}|$, and therefore

$$|E_T| \leq \frac{72046}{125T}.$$

Proposition 33 then gives

$$A_T \leq 1 - a + (6a-2)p + (2-6a)p^2 + (2-6a)p(1-p) + |E_T| = 1 - a + |E_T|.$$

Thus $A_T < 1$ for $T > 576368$, contradicting $A_T \geq 1$. □

7. Proof of Theorem 8

7.1. **The finite pentagon inequality.** Put

$$R_5 = \frac{1}{2\sin(\pi/5)}, \ u_j = R_5\left(\cos\frac{2\pi j}{5}, \sin\frac{2\pi j}{5}\right), \ s = u_1 - u_0.$$

The two copies of P_5 have vertex sets

$$B_0 = \{u_0, u_1, u_2, u_3, u_4\}, \ B_1 = \{u_0 + s, u_1 + s, u_2 + s, u_3 + s, u_4 + s\}.$$

After identifying the common point $u_0 + s = u_1$, label the nine distinct points by $v_0, \ldots, v_8$ in the order

$$v_i = u_i \ (0 \leq i \leq 4), \ v_{4+j} = u_j + s \ (1 \leq j \leq 4).$$

The identity $u_0 + s = u_1$ gives the common point. There is no other common point: a chord of this regular pentagon of length 1 is a side, and the five oriented side vectors are distinct, so $u_i - u_j = u_1 - u_0$ forces $(i,j) = (1,0)$ (with indices taken modulo 5). Within the two pentagons, the side pairs are $(0,1), (1,2), (2,3), (3,4), (4,0)$ and

$(1,5),(5,6),(6,7),(7,8),(8,1)$. For completeness, the calculation for pairs joining the two pentagons uses

$$R_5^2 = \frac{5+\sqrt{5}}{10},\ |u_i - (u_j + s)|^2 = |u_i - u_j - u_1 + u_0|^2,$$

and

$$\cos 0 = 1,\ \cos\frac{2\pi}{5} = \frac{\sqrt{5}-1}{4},\ \cos\frac{4\pi}{5} = -\frac{\sqrt{5}+1}{4}.$$

For $i \in \{0,1,2,3,4\}$ and $j \in \{1,2,3,4\}$, the unit pairs joining the two pentagons are

$$(i,j) = (1,1),(1,4),(2,2),(3,3),(4,4).$$

The first two are already the translated-pentagon sides $(1,5)$ and $(1,8)$; the other three give $(2,6),(3,7),(4,8)$. Thus the complete unit-pair list is

$$\mathcal{E}_5 = \{(0,1),(0,4),(1,2),(1,5),(1,8),(2,3),(2,6),\\ (3,4),(3,7),(4,8),(5,6),(6,7),(7,8)\}.$$

The corresponding index sets are

$$I_0 = \{0,1,2,3,4\},\ I_1 = \{1,5,6,7,8\}.$$

Write $x_i = 1$ when v_i is red and $x_i = 0$ when it is blue. A coloring with no red unit pair and no blue copy of P_5 must satisfy

$$x_i x_j = 0 \text{ for } (i,j) \in \mathcal{E}_5,$$
$$x_0 + x_1 + x_2 + x_3 + x_4 \geq 1,$$
$$x_1 + x_5 + x_6 + x_7 + x_8 \geq 1.$$

The first condition excludes red unit pairs. The last two conditions say that each pentagon contains a red point; otherwise that pentagon would be an all-blue copy of P_5.

For $x \in \{0,1\}^9$, define

$$\mathcal{F}_{P_5}(x) = -76 + \sum_i \alpha_i x_i + \sum_{i<j} \beta_{ij} x_i x_j,$$

where the coefficient vector and the upper-triangular matrix (β_{ij}) are listed in Table 12 in the appendix.

Lemma 34. *If no pair in $\mathcal{E}_5$ is simultaneously red and each pentagon contains a red point, then $\mathcal{F}_{P_5} \geq 1$.*

Proof. For $x = (x_0,\dots,x_8) \in \{0,1\}^9$, consider the vectors for which $x_i x_j = 0$ for $(i,j) \in \mathcal{E}_5$, $\sum_{i=0}^4 x_i \geq 1$, and $x_1 + x_5 + x_6 + x_7 + x_8 \geq 1$. There are 42 such colorings, and substitution into the polynomial gives $\mathcal{F}_{P_5}(x) \geq 1$ for each of them. □

7.2. **The pentagon kernel.** There are 36 quadratic pairs, but eight have zero coefficient. Computing the squared distances of the remaining 28 pairs in $\mathbb{Q}(\sqrt{5})$ and grouping their coefficients gives

squared distance	number of nonzero-coefficient pairs	coefficient sum
$\frac{3-\sqrt{5}}{2}$	3	200
1	13	-1048
$\frac{5-\sqrt{5}}{2}$	2	100
$\frac{3+\sqrt{5}}{2}$	10	$-385.$

Every nonzero quadratic coefficient occurs in one of these four classes; the eight zero coefficients contribute nothing. Hence these are the only squared distances with nonzero coefficient sum, and all other distance classes disappear from the kernel. Consequently,

$$K_5(t) = 200J_0\left(\sqrt{\frac{3-\sqrt{5}}{2}}\,t\right) - 1048J_0(t) + 100J_0\left(\sqrt{\frac{5-\sqrt{5}}{2}}\,t\right) - 385J_0\left(\sqrt{\frac{3+\sqrt{5}}{2}}\,t\right).$$

Proposition 35. *For every $t \geq 0$, $K_5(t) < 393$.*

Proof. On $[0, 12]$, Appendix A gives $K_5(\tau_k) < 389$ at the midpoints of a grid with spacing $1/200$, and $|K_5'| < 15949/12$. Hence the mean value theorem gives

$$K_5(t) < 389 + \frac{15949}{4800} < 393.$$

For $t \geq 12$, put $q_1 = (3-\sqrt{5})/2$, $q_3 = (5-\sqrt{5})/2$, and $q_4 = (3+\sqrt{5})/2$. Lemma 17 gives $|K_5(t)| \leq \sqrt{2/(\pi t)}\sum_i |c_i| q_i^{-1/4}$ for the four terms in K_5, with $q_2 = 1$. The bounds

$$q_1^{1/4} > \frac{39}{50}, \qquad q_3^{1/4} > \frac{27}{25}, \qquad q_4^{1/4} > \frac{127}{100}$$

give $\sum_i |c_i| q_i^{-1/4} < 1701$. Since $\pi > 3.14$ and $t \geq 12$, $\sqrt{2/(\pi t)} < 5/\sqrt{471}$, and therefore $|K_5(t)| < 392 < 393$. □

Proof of Theorem 8. Assume that a measurable coloring has no red unit pair and no blue copy of P_5. Let r be the red indicator, put $p = p_T(r)$, and set $f_T = r - p_T(r)$. The local lemma gives $A_T \geq 1$. Proposition 15 gives

$$A_T = -76 + 285p - 1133p^2 + \int_0^\infty K_5(t)\,\mathrm{d}\mu_{f,T}(t) + E_T,$$

where $\mu_{f,T}$ has mass $p(1-p)$. Since $\sum_i |\alpha_i| = 623$, $\sum_{i<j} |\beta_{ij}| = 2163$, and the patch has radius less than 2, Proposition 15 gives $|E_T| \leq 91504/T$. Using $K_5 < 393$,

$$A_T \leq -76 + 678p - 1526p^2 + \frac{91504}{T} \leq -\frac{1055}{1526} + \frac{91504}{T},$$

where the last inequality follows by completing the square. At $T = 200000$ the right side is negative, contradicting $A_T \geq 1$. $\square$

8. Proof of Theorem 9

8.1. The three-cube inequality. Put $e = (1,0,0)$ and define

$$\begin{aligned} v_0 &= (0,1,0), & w_0 &= (0,0,1), \\ v_1 &= (0,1/2,\sqrt{3}/2), & w_1 &= (0,-\sqrt{3}/2,1/2), \\ v_2 &= (0,-1/2,\sqrt{3}/2), & w_2 &= (0,-\sqrt{3}/2,-1/2). \end{aligned}$$

For $r \in \{0,1,2\}$, put $C_r = \{ae + bv_r + cw_r : a,b,c \in \{0,1\}\}$ and let $\mathcal{P} = C_0 \cup C_1 \cup C_2$. The definitions give $e \cdot v_r = e \cdot w_r = v_r \cdot w_r = 0$ and $|e| = |v_r| = |w_r| = 1$. Thus, for each r, the vectors e, v_r, w_r form an orthonormal basis, and C_r is the vertex set of a unit cube. The three cubes share the edge $\{0, e\}$, and their union $\mathcal{P}$ has twenty points.

Consider the Euclidean isometries

$$\tau(x,y,z) = (1-x,y,z)$$

and

$$\sigma(x,y,z) = \left(x, -\frac{\sqrt{3}}{2}y - \frac{1}{2}z, -\frac{1}{2}y + \frac{\sqrt{3}}{2}z\right),$$

and write $G = \langle \tau, \sigma \rangle$.

Label the points by

$$\begin{aligned} &p_0 = 0, && p_1 = w_0, && p_2 = v_0, && p_3 = v_0 + w_0, \\ &p_4 = e, && p_5 = e + w_0, && p_6 = e + v_0, && p_7 = e + v_0 + w_0, \\ &p_8 = w_1, && p_9 = v_1, && p_{10} = v_1 + w_1, && p_{11} = e + w_1, \\ &p_{12} = e + v_1, && p_{13} = e + v_1 + w_1, && p_{14} = w_2, && p_{15} = v_2, \\ &p_{16} = v_2 + w_2, && p_{17} = e + w_2, && p_{18} = e + v_2, && p_{19} = e + v_2 + w_2. \end{aligned}$$

The following classification is needed because the six pairwise distances do not by themselves characterize a square in three dimensions. For example, the points p_0, p_1, p_4, p_8 have four unit pairs and two pairs at distance $\sqrt{2}$, but

$$\det[p_1 - p_0,\ p_4 - p_0,\ p_8 - p_0] = -\frac{\sqrt{3}}{2} \neq 0.$$

They are noncoplanar and form a copy of $\mathcal{T}$.

Lemma 36. *Let $X \subset \mathbb{E}^3$ have four pairs at distance 1 and two pairs at distance $\sqrt{2}$. If the two pairs at distance $\sqrt{2}$ are disjoint, then X is a unit square; if they share a vertex, then X is isometric to $\mathcal{T}$.*

Proof. If the two $\sqrt{2}$-pairs are disjoint, label them $\{x_1, x_3\}$ and $\{x_2, x_4\}$. After translating the midpoint of x_1x_3 to the origin, $x_3 = -x_1$ and $|x_1|^2 = 1/2$. Since each of x_2, x_4 is at distance 1 from both x_1 and x_3, we have $x_1 \perp x_2, x_4$ and $|x_2|^2 = |x_4|^2 = 1/2$. The relation $|x_2 - x_4|^2 = 2$ then gives $x_4 = -x_2$. Thus $X = \{\pm x_1, \pm x_2\}$ with $x_1 \perp x_2$ and $|x_1| = |x_2| = 1/\sqrt{2}$, so X is a unit square.

If the pairs share a vertex, label the points $0, a, b, c$ so that $|a-b| = |b-c| = \sqrt{2}$. The other four distances are 1, so the Gram matrix of (a, b, c) is

$$\begin{pmatrix} 1 & 0 & 1/2 \\ 0 & 1 & 0 \\ 1/2 & 0 & 1 \end{pmatrix},$$

which is also the Gram matrix of $e_1, e_2, \frac{1}{2}e_1 + \frac{\sqrt{3}}{2}e_3$. A Gram matrix records all inner products after the common base point has been fixed, so two such lists of vectors are related by an orthogonal map on their spans; that map extends to an orthogonal map of $\mathbb{E}^3$. Thus Gram matrices determine the configuration up to Euclidean isometry, and X is isometric to $\mathcal{T}$. □

On the labels, the generators act as

$$\sigma = (1\ 15)(2\ 14)(3\ 16)(5\ 18)(6\ 17)(7\ 19)(8\ 9)(11\ 12),$$
$$\tau = (0\ 4)(1\ 5)(2\ 6)(3\ 7)(8\ 11)(9\ 12)(10\ 13)(14\ 17)(15\ 18)(16\ 19).$$

Lemma 37. *The set $\mathcal{P}$ has twenty points. Among its four-point subsets there are twenty-two copies of $\mathcal{S}$ and twenty-four copies of $\mathcal{T}$. Moreover, G has order four, preserves $\mathcal{P}$, and has fifty-six orbits on the unordered pairs of points of $\mathcal{P}$.*

Proof. All coordinates lie in $\mathbb{Q}(\sqrt{3})$. Appendix A.3 records the six squared distances for each of the $\binom{20}{4}$ four-point subsets. It identifies forty-six subsets whose six squared distances, counted with multiplicity, are $\{1, 1, 1, 1, 2, 2\}$. Among these, the two pairs at squared distance 2 are disjoint in twenty-two cases and share a vertex in twenty-four cases. Lemma 36 therefore identifies these cases as twenty-two copies of $\mathcal{S}$ and twenty-four copies of $\mathcal{T}$.

For $a, b, c \in \{0, 1\}$, the formulas defining τ and σ are

$$\tau(ae + bv_r + cw_r) = (1-a)e + bv_r + cw_r,$$

while $\sigma e = e$, $(\sigma v_0, \sigma w_0) = (w_2, v_2)$, $(\sigma v_1, \sigma w_1) = (w_1, v_1)$, and $(\sigma v_2, \sigma w_2) = (w_0, v_0)$. Thus τ preserves each C_r, while σ exchanges C_0 and C_2 and preserves C_1; both maps preserve $\mathcal{P}$. They are commuting Euclidean involutions, neither is the identity, and $\tau \neq \sigma$ since τ changes the first coordinate whereas σ fixes it. Thus G has order four. The induced action on the $\binom{20}{2} = 190$ unordered pairs has 2 orbits of size 1, 14 orbits of size 2, and 40 orbits of size 4. Hence there are 56 pair orbits, accounting for $2 \cdot 1 + 14 \cdot 2 + 40 \cdot 4 = 190$ pairs. □

Index the pair orbits by $\mathcal{O}_0, \ldots, \mathcal{O}_{55}$ in the order of the representatives in Appendix B; this row order is the definition of the indices. For a coloring encoded by $s : \mathcal{P} \to \{-1, 1\}$, define $X_j(s) = \sum_{\{p_u, p_v\} \in \mathcal{O}_j} s(p_u)s(p_v)$. Let a_j be the corresponding integer coefficient. Thus $X_j(s)$ is the sum of the products $s(p_u)s(p_v)$ over the pairs in the orbit in row j of Appendix B, and a_j is the coefficient in that same row. The symmetry reduction gives

$$\mathcal{L}_{\mathcal{S}}(s) = \frac{1}{1000}\left(-35608 + \sum_{j=0}^{55} a_j X_j(s)\right). \tag{8.1}$$

The four-point subsets in the local check are those whose six squared distances, counted with multiplicity, are $\{1,1,1,1,2,2\}$. Both a unit square and $\mathcal{T}$ have these six squared distances, and Lemma 36 says that every subset with these distances is one of these two configurations. Hence the forty-six forbidden subsets are the twenty-two copies of $\mathcal{S}$ and the twenty-four copies of $\mathcal{T}$ from Lemma 37.

Lemma 38. *If $s : \mathcal{P} \to \{-1,1\}$ contains neither a monochromatic copy of $\mathcal{S}$ nor a monochromatic copy of $\mathcal{T}$, then $\mathcal{L}_{\mathcal{S}}(s) \geq 1$.*

Proof. Let $R = \{p \in \mathcal{P} : s(p) = 1\}$ be the red set. Among the 2^{20} subsets $R \subseteq \mathcal{P}$, keep those for which no one of the forty-six forbidden four-point subsets is contained in R or in $\mathcal{P} \setminus R$. There are 47946 such subsets. Substitution of the integer coefficients from Appendix B gives the numerator at least 1000 in each case, and hence $\mathcal{L}_S(s) \geq 1$. □

We now average the local inequality. Suppose that a measurable red–blue coloring of $\mathbb{R}^3$ contains neither a monochromatic unit square nor a monochromatic copy of $\mathcal{T}$, and put $s = 1_R - 1_B : \mathbb{R}^3 \to \{-1,1\}$. For $x \in \mathbb{R}^3$, $U \in \mathrm{SO}(3)$, and $p \in \mathcal{P}$, put $s_{x,U}(p) = s(x+Up)$, and define

$$A_T = \frac{1}{|B_T|}\int_{\mathrm{SO}(3)}\int_{B_T} \mathcal{L}_S(s_{x,U})\,\mathrm{d}x\,\mathrm{d}U,$$

where $\mathrm{d}U$ is the probability measure on SO(3) invariant under rotations. Lemma 38 gives

$$A_T \geq 1. \tag{8.2}$$

For each squared distance q occurring in $\mathcal{P}$, define

$$B_q = \sum_{\substack{0 \leq j \leq 55 \\ |p_u - p_v|^2 = q \text{ on } \mathcal{O}_j}} |\mathcal{O}_j| a_j.$$

The coefficient sums B_q are listed in Table 17 in the appendix. In particular, $\sum_q |B_q| = 620268$. Define

$$K_S(t) = \frac{1}{1000}\left(-35608 + \sum_q B_q \Omega_3(\sqrt{q}\,t)\right). \tag{8.3}$$

Proposition 39. *There is a nonnegative measure $\nu_{s,T}$ on Fourier radii of mass 1 such that*

$$A_T = \int_0^\infty K_S(t)\,\mathrm{d}\nu_{s,T}(t) + O(T^{-1}).$$

For $T > 2\sqrt{3}$,

$$\left|A_T - \int_0^\infty K_S(t)\,\mathrm{d}\nu_{s,T}(t)\right| \leq \frac{401844\sqrt{3}}{25T}. \tag{8.4}$$

Proof. Take $\nu_{s,T}$ from Lemma 11. For a fixed pair $p_u, p_v \in \mathcal{P}$, the substitution $y = x + Up_u$ gives

$$\int_{B_T} s(x+Up_u)s(x+Up_v)\,\mathrm{d}x = \int_{B_T + Up_u} s(y)s(y + U(p_v - p_u))\,\mathrm{d}y.$$

Let $A = B_T + Up_u$ and $C = B_T \cap (B_T - U(p_v - p_u))$. Since $|p_u|, |p_v| \le \sqrt{3}$, both A and C contain $B_{T-2\sqrt{3}}$ and are contained in $B_{T+\sqrt{3}}$; in other words,

$$B_{T-2\sqrt{3}} \subseteq A \cap C \subseteq B_{T+\sqrt{3}}.$$

Thus

$$\frac{|A \triangle C|}{|B_T|} \le \frac{(T+\sqrt{3})^3 - (T-2\sqrt{3})^3}{T^3} \le \frac{9\sqrt{3}}{T} \le \frac{24\sqrt{3}}{T}.$$

The difference between the normalized integrals is therefore at most $24\sqrt{3}/T$. Averaging over U and applying Lemma 11 gives

$$\frac{1}{|B_T|} \int_{\mathrm{SO}(3)} \int_{B_T} s(x + Up_u) s(x + Up_v)\, \mathrm{d}x\, \mathrm{d}U = \int_0^\infty \Omega_3(|p_u - p_v| t)\, \mathrm{d}\nu_{s,T}(t) + O(T^{-1}).$$

Each pair in the orbit $\mathcal{O}_j$ carries the same coefficient a_j. Therefore the sum of the absolute coefficients over individual pairs is

$$\sum_{j=0}^{55} \sum_{\{p_u, p_v\} \in \mathcal{O}_j} |a_j| = \sum_{j=0}^{55} |\mathcal{O}_j|\, |a_j|.$$

From the coefficient data,

$$\sum_{j=0}^{55} |\mathcal{O}_j|\, |a_j| = 669740.$$

Consequently, after the factor $1/1000$ in (8.1), the total boundary error is at most $24\sqrt{3} \cdot 669740/(1000T) = 401844\sqrt{3}/(25T)$. Substituting the pair identities into (8.1) and grouping terms by the fourteen squared distances gives (8.3). Finally, $s^2 = 1$ pointwise, so

$$\nu_{s,T}([0,\infty)) = \frac{1}{|B_T|} \int_{B_T} s(x)^2\, \mathrm{d}x = 1.$$

□

8.2. **Bounds for the kernel.**

Proposition 40. *For every $t \ge 0$, one has $K_S(t) < 191/400 < 1$.*

Proof. Appendix A.3 gives the interval bound

$$K_S(j/1000) < \frac{3}{250} \tag{8.5}$$

on the grid with spacing $1/1000$ in $[0, 40]$. Every squared distance in (8.3) is less than 9. Lemma 10 gives $|\Omega_3'| \le 1/2$, so the chain rule gives $|K_S'(t)| \le (1/2000) \sum_q |B_q| \sqrt{q} < 931$.

If $0 \le t \le 40$, choose j with $|t - j/1000| \le 1/2000$. The mean value theorem and (8.5) give $K_S(t) < 3/250 + 931/2000 = 191/400$.

Now suppose $t \ge 40$. The smallest squared distance in the kernel is $2 - \sqrt{3} > 1/4$, so every corresponding distance is greater than $1/2$ and every argument $\sqrt{q}\, t$ is greater than $20 > 2$. Thus the large-argument estimate $|\Omega_3(u)| \le 1/u$ from Lemma 17 applies and gives

$$K_S(t) \le -\frac{35608}{1000} + \frac{2 \cdot 620268}{1000t} \le -\frac{22973}{5000} < \frac{191}{400}.$$

□

Proof of Theorem 9. Suppose that a measurable red–blue coloring of $\mathbb{R}^3$ contains neither a monochromatic unit square nor a monochromatic copy of $\mathcal{T}$. Equation (8.2) gives $A_T \geq 1$. On the other hand, Proposition 39, the positivity and unit mass of $\nu_{s,T}$, and Proposition 40 give

$$A_T \leq \frac{191}{400} + \frac{401844\sqrt{3}}{25T}.$$

Since $A_T \geq 1$ while $1 - 191/400 = 209/400$, the upper bound is less than 1 whenever

$$\frac{401844\sqrt{3}}{25T} < \frac{209}{400} \iff T > \frac{401844 \cdot 400}{25 \cdot 209}\sqrt{3} = \frac{6429504}{209}\sqrt{3}.$$

This contradiction proves Theorem 9. □

9. Linear programs

The finite inequalities above were found with linear programs. We record the formulations because they make the role of the coefficients transparent. The LPs are used to choose real coefficients; after rounding, the proofs use the resulting rational or integer data. The local inequalities are then checked on the finite sets of colorings and sequences, while the bounds for all $t \geq 0$ follow from the analytic estimates in the proof sections. The objective in each LP is to maximize a gap δ between the local lower bound and the averaged upper bound.

We count scalar inequalities and equalities separately; a two-sided bound on a variable contributes two inequalities. For each LP, let $\mathcal{N}$ denote the finite set of kernel sampling conditions used in its construction. In the planar quadratic LPs an element of $\mathcal{N}$ may include the density parameter as well as the frequency. The sampling sets for the main kernel constraints are

$$\begin{aligned}
\mathcal{N}_7 &= \{j/400 : 0 \leq j \leq 40000\}, & \mathcal{N}_3 &= \{j/400 : 0 \leq j \leq 10000\},\\
\mathcal{N}_{34} &= \{j/5000 : 0 \leq j \leq 30000\}, & \mathcal{N}_{35} &= \{j/2000 : 0 \leq j \leq 50000\},\\
\mathcal{N}_{36} &= \{j/10000 : 0 \leq j \leq 100000\}, & \mathcal{N}_{44} &= \{j/2500 : 0 \leq j \leq 62500\},\\
\mathcal{N}_{\mathcal{S},\mathcal{T}} &= \{j/1000 : 0 \leq j \leq 40000\}.
\end{aligned}$$

For $W_4(\sqrt{2})$ and P_5, write $\mathcal{N}_{W_4(\sqrt{2})}$ and $\mathcal{N}_{P_5}$ for the finite sets of sampled (p,t) pairs used in their quadratic LPs. Their cardinalities, together with the dimensions and scalar constraint counts of all nine LPs, are recorded in Appendix A. The sampled constraints are used only to select the coefficients; the proofs use the rounded data and the separate analytic checks below.

9.1. **Planar quadratic inequalities.**

We first describe the common planar setup. Let V be a finite point set, let $B_1, \ldots, B_s \subseteq V$ be the local copies of the target configuration, and let E be the set of forbidden unit pairs. Write $r_v \in \{0,1\}$ for the indicator that v is red. The allowed local colorings are the vectors $r = (r_v)_{v \in V}$ satisfying

$$r_u r_v = 0 \text{ for } \{u,v\} \in E, \sum_{v \in B_i} r_v \geq 1 \text{ for } 1 \leq i \leq s.$$

The first condition excludes a red unit pair, and the second says that each local copy has a red point, so that it is not all blue. For LP coefficients c, a_v, and $b_{uv} = b_{vu}$, consider

$$\widetilde{\mathcal{L}}(r) = c + \sum_{v\in V} a_v r_v + \sum_{\{u,v\}\subseteq V} b_{uv} r_u r_v.$$

For a measurable global red indicator, write $p = p_T(r)$ and $f_T = r - p_T(r)$. For $0 < p < 1$, normalize the measure on Fourier radii associated with the centered function f_T by its mass $p(1-p)$. At a fixed frequency t, the contribution of the term $r_u r_v$ in the rotationally averaged correlation is

$$p^2 + p(1-p)J_0(|u-v|t).$$

The full average integrates this expression against the normalized nonnegative measure on Fourier radii; it is not obtained by evaluating it at a single frequency. If $p = 0$ or $p = 1$, the centered measure is zero and the pair contribution is simply p^2. Since the measure is nonnegative, pointwise bounds in p and t are enough. Here J_0 is the Bessel function of order zero. Thus the averaged expression is

$$\widetilde{H}(p,t) = c + p\sum_{v\in V} a_v + \sum_{\{u,v\}\subseteq V} b_{uv}\Big(p^2 + p(1-p)J_0(|u-v|t)\Big).$$

The corresponding LP has variables $\delta, c, (a_v)_{v\in V}, (b_{uv})_{\{u,v\}\subseteq V}$ and objective maximize δ, subject to

$$\begin{array}{ll}
\text{maximize} & \delta \\
\text{variables} & \delta, c, (a_v)_{v\in V}, (b_{uv})_{\{u,v\}\subseteq V} \\
\text{subject to} & \widetilde{\mathcal{L}}(r) \geq 1 \text{ for every allowed coloring } r, \\
 & \widetilde{H}(p,t) \leq 1-\delta \text{ for every sampled pair } (p,t), \\
 & 0 \leq \delta \leq 100, \\
|c|, |a_v|, |b_{uv}| \leq 100. &
\end{array}$$

The coefficient of each variable is fixed by the local geometry and the chosen samples. For $W_4(\sqrt{2})$ and P_5, the point sets have respectively 8 and 9 points, so the quadratic LPs have $2 + 8 + \binom{8}{2} = 38$ and $2 + 9 + \binom{9}{2} = 47$ variables, respectively. Their numbers of allowed colorings and kernel inequalities are given in Table 5.

The eighteen-point and nine-point planar inequalities use the same principle, with symmetry and color indicators reducing the number of variables. For the eighteen-point configuration, let N_R and N_B count red and blue points, and let $\mathcal{A}_7$ be the set of colorings with no red unit pair and no blue copy of ℓ_7. For variables x_v and $y_{uv} = y_{vu}$, define

$$\begin{aligned}
\widetilde{\mathcal{L}}_7(r) &= -1000 + \frac{500}{9}N_R + \frac{500}{9}N_B + \sum_v x_v r_v + \sum_{\{u,v\}} y_{uv} r_u r_v, \\
\widetilde{H}_R(t) &= 1000 + \sum_v x_v + \sum_{\{u,v\}} y_{uv} J_0(|u-v|t), \\
\widetilde{H}_B(t) &= 1000,
\end{aligned}$$

The two indicator measures make the averaging behind this formulation explicit. If p is the red density, then, apart from the boundary error,

$$\widetilde{A}_{7,T} = -1000 + \int_0^\infty \widetilde{H}_R(u)\,\mathrm{d}\nu_{r,T}(u) + \int_0^\infty \widetilde{H}_B(u)\,\mathrm{d}\nu_{b,T}(u) + O(T^{-1}).$$

The corresponding centered (p,t) expression, after the constant linear terms cancel, is

$$\widetilde{\mathcal{H}}_7(p,t) = p\sum_v x_v + p^2 \sum_{\{u,v\}} y_{uv} + p(1-p)\sum_{\{u,v\}} y_{uv} J_0(|u-v|t).$$

The two measures in the preceding average have masses p and $1-p$. The LP below optimizes only the red kernel $\widetilde{H}_R$ against the fixed reference value $\widetilde{H}_B = 1000$. This is the pointwise kernel bound used in the proof, while the expression above records its relation to the full average.

The LP is

$$\begin{array}{ll} \text{maximize} & \delta \\ \text{variables} & \delta,\ (x_v)_{v\in P},\ (y_{uv})_{\{u,v\}\subseteq P} \\ \text{subject to} & \widetilde{\mathcal{L}}_7(r) \geq 1 \text{ for } r \in \mathcal{A}_7, \\ & \widetilde{H}_R(t) \leq 1000 - \delta \text{ for } t \in \mathcal{N}_7. \end{array}$$

This LP has $172 = 1 + 18 + 153$ variables and 751 local inequalities. The number of kernel inequalities is given in Table 5; the remaining range $t \geq 100$ is covered by the Bessel estimate in the proof of the eighteen-point kernel proposition.

The nine-point three-color LP has variables δ, four vertex-orbit coefficients, and thirteen coefficients for each of two types of pair sums, for a total of $31 = 1+4+13+13$ variables. If $\mathcal{A}_3$ denotes the 304 colorings satisfying its local conditions, its local expression is

$$\widetilde{\mathcal{L}}_3 = -196 + \sum_O x_O [g]_O + \sum_U \Big(y_U [gg]_U + z_U [ss]_U \Big),$$

with averaged expressions

$$\widetilde{H}_g(t) = \sum_O x_O + \sum_U y_U J_0(\sqrt{d(U)}t),$$
$$\widetilde{H}_s(t) = \sum_U z_U J_0(\sqrt{d(U)}t).$$

In terms of the two measures, the averaged expression is

$$\widetilde{A}_{3,T} = -196 + \int_0^\infty \widetilde{H}_g(t)\,\mathrm{d}\nu_{g,T}(t) + \int_0^\infty \widetilde{H}_s(t)\,\mathrm{d}\nu_{s,T}(t) + O(T^{-1}),$$

and the two nonnegative measures have masses whose sum is 1. Thus $\widetilde{H}_g$ and $\widetilde{H}_s$ are the two averaged kernels, including the constant term in $\widetilde{H}_g$; the LP optimizes their common pointwise upper bound rather than a separate density parameter.

The LP is

$$\begin{array}{ll} \text{maximize} & \delta \\ \text{variables} & \delta,\ (x_O)_O,\ (y_U)_U,\ (z_U)_U \\ \text{subject to} & \widetilde{\mathcal{L}}_3(r) \geq 0 \text{ for } r \in \mathcal{A}_3, \\ & \widetilde{H}_g(t) \leq 196 - \delta \text{ for } t \in \mathcal{N}_3, \\ & \widetilde{H}_s(t) \leq 196 - \delta \text{ for } t \in \mathcal{N}_3. \end{array}$$

The LP has $31 = 1 + 4 + 13 + 13$ variables and 304 local inequalities. The number of kernel inequalities is given in Table 5. The common bound for $\widetilde{H}_g$ and $\widetilde{H}_s$ is needed because the two associated measures have total mass 1.

9.2. **Linear programs for the line graphs.** For the four higher-dimensional line results, the finite object is a directed graph of allowed local sequences rather than a point configuration. Let $\mathcal{T}_q$ be its directed edge set, with initial and terminal vertices $u(z)$ and $v(z)$. The LP variables are the coefficients in a local expression $\widetilde{W}_q$, the potential values $\widetilde{\phi}_q(u)$ on the vertices, and the gap δ_q. The local constraints are

$$\widetilde{W}_q(z) + \widetilde{\phi}_q(u(z)) - \widetilde{\phi}_q(v(z)) \geq 0 \text{ for } z \in \mathcal{T}_q.$$

The four local expressions used in the LPs are

$$\begin{aligned}
\widetilde{W}_{34}(r) &= -1 + a_{34}r_0 + c_{34,1}r_0r_1 + c_{34,2}r_0r_2,\\
\widetilde{W}_{35}(r) &= -6 + a_{35}r_0 + \sum_{k=1}^{6} c_{35,k}r_0r_k,\\
\widetilde{W}_{36}(r) &= -2 + a_{36}r_0 + \sum_{k\in\{1,2,4,5,6\}} c_{36,k}r_0r_k,\\
\widetilde{W}_{44}(s) &= -1 + \sum_{k=1}^{4} c_{44,k}s_0s_k.
\end{aligned}$$

Writing Ω_d for the spherical averaging function in dimension d, put $p = p_T(r)$ and $f_T = r - p_T(r)$. The associated kernel expressions are $\widetilde{H}_q(t) = \sum_k c_{q,k}\Omega_{d_q}(kt)$. The fixed local constants and the linear terms are not part of $\widetilde{H}_q$. For $q = 34, 35, 36$, the full averaged expression has the form

$$\widetilde{\mathcal{L}}_{q,T} = \alpha_q + \beta_q p + S_q p^2 + \int_0^\infty \widetilde{H}_q(t)\,\mathrm{d}\mu_{f,T}(t) + O(T^{-1}),$$

where

q	α_q	β_q	S_q
34	-1	4	-5
35	-6	28	-37
36	-2	11	-16

and $\mu_{f,T}$ has mass $p(1-p)$. For $q = 44$, the signed-function identity is

$$\widetilde{\mathcal{L}}_{44,T} = -1 + \int_0^\infty \widetilde{H}_{44}(t)\,\mathrm{d}\nu_{s,T}(t) + O(T^{-1}), \text{ and } \nu_{s,T}([0,\infty)) = 1.$$

Thus these line LPs optimize only the pointwise kernel bounds $\widetilde{H}_q(t) \leq B_q - \delta_q$ for $t \in \mathcal{N}_q$. The polynomials in the color density in the first display are handled separately by completing the square in the theorem proofs; the LP does not optimize those polynomials over p. The sample sets and upper bounds are

q	d_q	B_q
34	3	7/10
35	4	59/20
36	7	2/5
44	4	9/10

For definiteness, impose the bounds

$$-100 \leq \delta_q \leq 100, |a_q|, |c_{q,k}| \leq 100, |\widetilde{\phi}_q(u)| \leq 1000.$$

The variable a_q is omitted when $q = 44$. These bounds make the LP bounded; the proofs use only the rounded coefficients and potentials.

For each row q, choose a vertex u_q^* and impose the normalization $\widetilde{\phi}_q(u_q^*) = 0$. The four LPs can then be written together as

$$\begin{array}{ll} \text{maximize} & \delta_q \\ \text{variables} & \delta_q,\ a_q,\ (c_{q,k})_k,\ (\widetilde{\phi}_q(u))_u \\ \text{subject to} & \widetilde{W}_q(z) + \widetilde{\phi}_q(u(z)) - \widetilde{\phi}_q(v(z)) \geq 0 \text{ for } z \in \mathcal{T}_q, \\ & \widetilde{H}_q(t) \leq B_q - \delta_q \text{ for } t \in \mathcal{N}_q, \\ & \widetilde{\phi}_q(u_q^*) = 0, \\ & -100 \leq \delta_q \leq 100, \\ & |a_q|, |c_{q,k}| \leq 100, \\ & |\widetilde{\phi}_q(u)| \leq 1000. \end{array}$$

In the (ℓ_4, ℓ_4) row, the variable a_q is omitted. The numbers of variables and all scalar constraint counts are collected in Table 5; the sample sets $\mathcal{N}_q$ are specified above.

The rounded variable coefficients are

q	a_q	$(c_{q,k})_k$
34	4	$(-3, -2)$
35	28	$(-20, -14, -3, -4, 2, 2)$
36	11	$(-9, -5, -2, -1, 1)$ for $k = 1, 2, 4, 5, 6$
44	–	$(-6, -4, -2, 1)$.

The corresponding integer-valued functions ϕ_q complete the four rounded inequalities. The local and kernel checks use the rounded data, not the numerical solutions of the LPs.

9.3. **The square–tetrahedron LP.** The square–tetrahedron LP uses signs $s_v \in \{-1, 1\}$ on the twenty-point configuration and groups the 56 pair terms into orbits under the configuration symmetries. For each orbit, let $X_j(s)$ be the sum of the products of the signs on its pairs. The local expression and its averaged kernel are

$$\widetilde{\mathcal{L}}_{\mathcal{S},\mathcal{T}}(s) = c + \sum_{j=0}^{55} b_j X_j(s), \widetilde{K}_{\mathcal{S},\mathcal{T}}(t) = c + \sum_{j=0}^{55} |\mathcal{O}_j| b_j \Omega_3(\sqrt{q_j}\, t).$$

Let $\mathcal{A}_{\mathcal{S},\mathcal{T}}$ be the set of the 47946 sign colorings $s : \mathcal{P} \to \{-1, 1\}$ that avoid both monochromatic configurations. The LP is

$$\begin{array}{ll} \text{maximize} & \delta \\ \text{variables} & \delta, c, (b_j)_{0 \le j \le 55} \\ \text{subject to} & \widetilde{\mathcal{L}}_{\mathcal{S},\mathcal{T}}(s) \ge 1 \text{ for } s \in \mathcal{A}_{\mathcal{S},\mathcal{T}}, \\ & \widetilde{K}_{\mathcal{S},\mathcal{T}}(t) \le 1 - \delta \text{ for } t \in \mathcal{N}_{\mathcal{S},\mathcal{T}}, \\ & |c| \le 50 \text{ and } |b_j| \le 50 \text{ for } 0 \le j \le 55. \end{array}$$

These are the colorings that avoid the twenty-two four-point subsets forming squares and the twenty-four four-point subsets forming copies of $\mathcal{T}$, as classified by the three-cube geometry lemma.

It has $58 = 1 + 1 + 56$ variables. There are 47946 allowed sign colorings, and the dimensions and scalar constraint counts are given in Table 5. The bounds on c and the b_j only make the LP bounded; they play no role in the mathematical statement.

10. Further consequences and open problems

10.1. **Further consequences.** The same local inequalities also give finite-ball versions. For $R > 0$, let $B_R^d = \{x \in \mathbb{E}^d : |x| \le R\}$. For finite configurations $X_1, \ldots, X_r \subset \mathbb{E}^d$, write $B_R^d \to_{\mathrm{m}} (X_1, \ldots, X_r)$ if every measurable coloring $B_R^d = C_1 \sqcup \cdots \sqcup C_r$ contains, for some i, an isometric copy of X_i all of whose points lie in C_i.

Corollary 41. *The following eight finite-ball relations hold with the indicated radii:*

$$\begin{array}{ll} B_R^2 \to_{\mathrm{m}} (\ell_2, \ell_7) & \textit{if } R > \frac{109469}{2}\sqrt{73}, \\ B_R^2 \to_{\mathrm{m}} (\ell_2, \ell_2, \ell_3) & \textit{if } R > \frac{134275}{3}\sqrt{3}, \\ B_R^3 \to_{\mathrm{m}} (\ell_3, \ell_4) & \textit{if } R > \frac{930453}{71}, \\ B_R^4 \to_{\mathrm{m}} (\ell_3, \ell_5) & \textit{if } R > \frac{899995754}{359}, \\ B_R^7 \to_{\mathrm{m}} (\ell_3, \ell_6) & \textit{if } R > \frac{130780346}{31}, \\ B_R^4 \to_{\mathrm{m}} (\ell_4, \ell_4) & \textit{if } R > 24324, \\ B_R^2 \to_{\mathrm{m}} (\ell_2, W_4(\sqrt{2})) & \textit{if } R > 576370, \\ B_R^2 \to_{\mathrm{m}} (\ell_2, P_5) & \textit{if } R > 200002. \end{array}$$

Moreover, if $R > \frac{6429713}{209}\sqrt{3}$, every measurable two-coloring of B_R^3 contains a monochromatic copy of $\mathcal{S}$ or a monochromatic copy of $\mathcal{T}$.

Proof. Repeat the corresponding averaging proof over B_T^d, extending the color indicators by zero outside B_R^d. It is enough that every translated local configuration used in the average remain inside B_R^d. Thus we may take $T = R - \rho$, where, in order, the required values of ρ are $\frac{\sqrt{73}}{2}$, $\sqrt{3}$, 3, 6, 6, 4, 2, 2, and $\sqrt{3}$. The first two values are the radii of the planar patches; the next four are the largest shifts along the local line; the two polygon patches have radius at most 2; and every point of the square–tetrahedron patch has norm at most $\sqrt{3}$.

The corresponding arguments give contradictions whenever

$$\begin{aligned} &T > 54734\sqrt{73}, && T > \frac{134272}{3}\sqrt{3}, && T > \frac{930240}{71}, \\ &T > \frac{899993600}{359}, && T > \frac{130780160}{31}, && T > 24320, \\ &T > 576368, && T > 200000, && T > \frac{6429504}{209}\sqrt{3}. \end{aligned}$$

Adding the corresponding value of ρ gives the stated radii. $\square$

Corollary 42. *For each of the first eight relations among the nine theorems above, every measurable coloring has a color class containing infinitely many pairwise disjoint isometric copies of the corresponding configuration. Moreover, every measurable two-coloring of $\mathbb{E}^3$ contains infinitely many pairwise disjoint monochromatic copies of at least one of $\mathcal{S}$ and $\mathcal{T}$.*

Proof. For one of the first eight relations, choose infinitely many pairwise disjoint balls with a radius satisfying its finite-radius bound. Restrict the coloring to each ball and apply Corollary 41, after translating the ball to B^d_R. Each ball then contains one of the finitely many color–configuration pairs (i, X_i). By the pigeonhole principle, one such pair occurs in infinitely many balls. The corresponding copies are pairwise disjoint because they lie in pairwise disjoint balls.

For the square–tetrahedron result, use balls with the corresponding finite radius. Each ball contains a monochromatic copy of $\mathcal{S}$ or of $\mathcal{T}$. There are only four choices of color and configuration, so one choice occurs in infinitely many balls. The corresponding copies are pairwise disjoint. $\square$

10.2. **An explicit polygon obstruction.** The general distance-avoiding-set theorem of Currier, Mody, Xie, and Zhang has an implicit constant in fixed dimension. Their planar argument for lines, however, keeps the relevant constants explicit. The same argument gives the following auxiliary obstruction for regular polygons.

Proposition 43. *Let P_N be the regular N-gon of side length one. For every integer $N \geq 6800$,*

$$\mathbb{E}^2 \nrightarrow (\ell_2, P_N).$$

Proof. Fix an integer $N \geq 6800$. We construct a periodic coloring with no red copy of ℓ_2 and no blue copy of P_N. We use the periodic cell construction of [10]. We first record the two estimates from that construction that will be used below. If $M \geq 4$ affine hyperplanes are given in $\mathbb{R}^4$, the number of their sign patterns, with zero signs included, is at most

$$\left(\frac{50M}{4}\right)^4. \tag{10.1}$$

This is the degree-one case of Theorem 2.3 of [10]. We also use the following form of Janson's inequality. If $X_1, \ldots, X_m$ are indicator variables with a dependency graph, and

$$\mu = \sum_i \mathbb{E}X_i,$$
$$\Delta = \sum_{i\sim j} \mathbb{E}(X_iX_j),$$
$$\delta = \max_i \sum_{j\sim i} \mathbb{E}X_j,$$

where the sum defining Δ is over unordered pairs, then

$$\mathbb{P}\left(\sum_i X_i = 0\right) \le \exp\Big(-\mu + \Delta e^{2\delta}\Big). \tag{10.2}$$

See Janson [22, Theorem 2].

Let Λ be the lattice generated by $(1-\varepsilon)(3/2,0)$ and $(1-\varepsilon)(3/4,\sqrt{3}/4)$, where $0<\varepsilon<1/100$. Its Voronoi cells are regular hexagons of diameter $1-\varepsilon<1$, and the shortest nonzero vector of Λ has length $(1-\varepsilon)\sqrt{3}/2 > 1/2$. Set $L = 3N$ and work on the torus $\mathbb{E}^2/L\Lambda$. Fix a total order on the finitely many cells of this torus, for example the lexicographic order induced by a chosen set of lattice representatives. Replace each closed Voronoi cell D by

$$D^* = D \setminus \bigcup_{D'\prec D} D'.$$

The sets D^* form a measurable half-open partition. Thus every point on a cell boundary is assigned to the $\prec$-least incident cell.

For a cell D, let $z(D)$ be the set of other cells whose distance from D is at most one. The hexagonal geometry gives $|z(D)| = 18$. Choose each cell independently with probability $p = 1/27$, and color D red if it was chosen and none of the cells in $z(D)$ was chosen; color all remaining points blue. Extend this coloring periodically to $\mathbb{E}^2$. If two points at distance one lay in red cells, their cells would be distinct and at distance at most one, contradicting the rule defining the red cells. Thus there is no red copy of ℓ_2.

We next count the sets of cells that can contain a copy of P_N. Since L times the shortest vector length is greater than $N+1$ and $\operatorname{diam}(P_N) \le N-1$, the vertices of every copy of P_N on the torus lie in distinct cells. Choose a centered fundamental parallelogram P_0. Its radius is less than $7N/2$: the distances from its center to its vertices are $L(1-\varepsilon)\sqrt{21}/4$ and $L(1-\varepsilon)\sqrt{3}/4$, and $3\sqrt{21}/4 < 7/2$. Lift a copy so that one vertex lies in P_0. Every lifted vertex, together with its cell, then lies in the ball of radius $5N$ about the origin.

The walls of these hexagonal cells lie in three families of parallel lines, with adjacent lines in each family at distance at least $1/3$. Consequently, the walls meeting the ball of radius $5N$ lie on at most $100N$ lines.

Fix two adjacent vertices q_1, q_2 of a labeled copy of P_N. For either orientation of the polygon, every other vertex has the form

$$q_i = q_1 + a_i(q_2 - q_1) + b_i J(q_2 - q_1),$$

where $J(x,y) = (-y,x)$ and a_i, b_i depend only on P_N and the chosen orientation. Each wall therefore gives an affine hyperplane in the four coordinates of (q_1,q_2). Across all N vertices there are at most $100N^2$ such hyperplanes. Their sign pattern determines the assigned cell of every vertex: zero signs identify the incident cells when a vertex lies on a wall, and the fixed tie-breaking rule then selects the $\prec$-least one. By (10.1), the number of such sets of cells for either orientation is at most

$$\left(\frac{50 \cdot 100N^2}{4}\right)^4 = 2^4 5^{16} N^8.$$

Thus the total number of such sets of cells is at most

$$2^5 5^{16} N^8. \tag{10.3}$$

It remains to bound the probability that one fixed set of cells is all blue. Write

$$d_k(N) = \frac{\sin(k\pi/N)}{\sin(\pi/N)}$$

for the distance between vertices separated by k sides. For $x = \pi/N$,

$$d_5(N) = 5 - 20\sin^2 x + 16\sin^4 x < 5.$$

Moreover, since $N \geq 19$ gives $6x < 1$ and $x < 1/6$,

$$d_6(N) = \frac{\sin(6x)}{\sin x} \geq 6 - 36x^2 > 5,$$

where we used $\sin y \geq y - y^3/6$ for $0 \leq y \leq 1$ and $\sin x \leq x$. The distances increase with k up to $N/2$, so each vertex has at most ten other vertices at distance less than five. The N pairs of adjacent vertices have distance one and cannot both lie in red cells. Hence, among all dependent pairs, at most $4N$ can have a nonzero joint red event.

Let X_i indicate that the cell containing the ith vertex is red, and put $a = (1-p)^{18}$. If two vertices are at distance at least five, the sets of cells determining their red events are disjoint. A common cell would, by the triangle inequality and the fact that every cell has diameter less than one, place the two vertices at distance less than five. Thus the relation $i \sim j$ defined by distance less than five is a dependency graph.

For a fixed set of cells, $\mathbb{E}X_i = pa$. If a nonadjacent dependent pair is red, both cells must be chosen and all cells in the union of their two z-sets must be unchosen; therefore $\mathbb{E}(X_i X_j) \leq p^2 a$. It follows that

$$\mu = Npa,$$
$$\Delta \leq 4Np^2 a,$$
$$\delta \leq 10pa.$$

Applying (10.2) gives

$$\mathbb{P}(X_1 = \cdots = X_N = 0) \leq \exp\Bigl(-Npa + 4Np^2 a\, e^{20pa}\Bigr). \tag{10.4}$$

We now make the numerical bound rational. For $p = 1/27$,

$$\frac{506958}{10^6} < a = \left(\frac{26}{27}\right)^{18} < \frac{506959}{10^6},$$
$$\frac{20a}{27} < \frac{939}{2500}.$$

The exponential series, with its tail bounded by a geometric series, gives

$$e^{20a/27} \leq \sum_{j=0}^{6} \frac{(939/2500)^j}{j!} + \frac{(939/2500)^7}{7!\,(1-939/20000)} < \frac{73}{50}.$$

Consequently,

$$-pa + 4p^2 a\, e^{20pa} < -\frac{506958}{27\cdot 10^6} + \frac{4\cdot 506959\cdot 73}{27^2\cdot 50\cdot 10^6} = -\frac{67045159}{4556250000} < -\frac{147}{10000}.$$

Combining this with (10.4), the probability that a fixed set of cells is all blue is at most $\exp(-147N/10000)$.

Let Z be the number of sets of cells from (10.3) that are all blue. Then

$$\mathbb{E}Z \leq 2^5 5^{16} N^8 \exp\left(-\frac{147N}{10000}\right).$$

The logarithm of the right-hand side is decreasing for $N \geq 6800$, since its derivative is $8/N - 147/10000 < 0$. At $N = 6800$, the following elementary logarithm bounds hold:

$$\log 2 < \frac{3466}{5000}, \quad \log 5 < \frac{3219}{2000}, \quad \log 6800 < \frac{88247}{10000}.$$

These rational estimates follow from $\log((1+z)/(1-z)) = 2\sum_{k\geq 0} z^{2k+1}/(2k+1)$, bounding the remaining positive tail by a geometric series. They give

$$\log(2^5 5^{16} 6800^8) < \frac{249539}{2500} < \frac{4991}{50},$$

whereas

$$\frac{147\cdot 6800}{10000} = \frac{2499}{25} = \frac{4998}{50}.$$

Thus $\mathbb{E}Z < e^{-7/50} < 1$ when $N = 6800$. Since the upper bound is decreasing for $N \geq 6800$, the same inequality holds for every such N. For the fixed integer N, choose the random cells so that $Z = 0$. The resulting periodic coloring has no blue copy of P_N and no red copy of ℓ_2. This proves the proposition. □

10.3. **Open problems.** The results suggest three broad questions.

Problem 1. *Can the measurability assumption be removed from the results of this paper? Equivalently, do all nine Ramsey relations proved here hold for arbitrary colorings? In particular, is the relation in Theorem 1 true without the measurable hypothesis?*

Problem 2. *Can the gaps between the known positive and negative results be narrowed? In particular:*

(i) does $\mathbb{E}^2 \to_{\mathrm{m}} (\ell_2, \ell_8)$ hold?
(ii) can any of the dimensions in Theorems 3–6 be lowered?
(iii) does $\mathbb{E}^3 \to_{\mathrm{m}} (\mathcal{S}, \mathcal{S})$ hold?
(iv) does $\mathbb{E}^2 \to_{\mathrm{m}} (\ell_2, P_7)$ hold?

Problem 3. *Can the finite-ball relations in Corollary 41 be proved with smaller radii?*

Appendix A. Finite checks

The coefficient data are recorded in Appendix B. The finite local inequalities are checked by enumeration. On bounded frequency intervals, the programs evaluate the relevant series with rational arithmetic (planar and line cases) or outward-rounded interval arithmetic (square–tetrahedron case); derivative bounds extend the checked values between sample points.

A.1. **Finite local checks.** The local checks are exhaustive and use only the rational or integer data in Appendix B; they do not use the numerical solutions of the LPs. For the eighteen-point configuration, enumerate the red subsets $R \subseteq P$ satisfying the local restrictions and evaluate the integer polynomial

$$F(R) = \sum_{p \in P} c_p r_p(R) + \sum_{\{p,q\} \subset P} a_{pq} r_p(R) r_q(R),$$

after the constant terms cancel. There are 751 allowed subsets, and evaluating $F(R)$ gives $F(R) \geq 1$ for every one of them.

For the nine-point three-color configuration, the local restrictions leave 304 colorings. With $g = 1_G$ and $s = 1_R - 1_B$, evaluating the integer expression $F = 4\mathcal{L}$ from the preceding lemma gives $F \geq 0$.

For the four line graphs, the allowed binary sequences have lengths $3, 6, 6, 4$. Their forbidden consecutive patterns and the numbers of vertices and edges are as follows. Join

case	forbidden consecutive patterns	vertices	edges
(ℓ_3, ℓ_4)	111, 0000	7	12
(ℓ_3, ℓ_5)	111, 00000	41	73
(ℓ_3, ℓ_6)	111, 000000	43	78
(ℓ_4, ℓ_4)	1111, 0000	14	26

Table 1. Sizes of the four finite line graphs.

two sequences when their overlapping entries agree and the resulting lengthened sequence contains no forbidden pattern. Substituting the integer potentials in Appendix B gives $W_q + \phi_q(u) - \phi_q(v) \geq 0$ for every resulting edge.

For $W_4(\sqrt{2})$, the local restrictions leave 37 binary colorings, and the integer numerator $1000\mathcal{F}_{W_4(\sqrt{2})}$ is at least 1000 on each of them.

For P_5, the local restrictions leave 42 binary colorings; substituting into the stated integer polynomial gives minimum 1.

A.2. **Bounded-interval check for the** (ℓ_2, ℓ_7) **kernel.** The distance classes contributing to H_R are listed below. Here m_q is the number of unordered pairs at squared distance q, and A_q is the sum of their coefficients. The two remaining squared distances, 64 and 73, have coefficient sum zero and do not appear in H_R.

To verify the estimate on the bounded interval, let

$$\mathcal{Q} = \{1, 3, 4, 7, 9, 13, 16, 21, 25, 31, 36, 43, 49, 57\}, K(t) = -319 + \sum_{q \in \mathcal{Q}} A_q J_0(\sqrt{q}\, t),$$

q	m_q	A_q
1	33	-489
3	15	1035
4	14	-669
7	13	600
9	12	-700
13	11	548
16	10	-355
21	9	441
25	8	-105
31	7	339
36	6	-114
43	5	-139
49	4	16
57	3	-90

TABLE 2. Distance classes and coefficient sums for H_R.

where the values A_q are listed in Table 2. Evaluate the Bessel series with rational interval bounds successively at rational left endpoints. If K_i^+ is the resulting rational upper bound for $K(t_i)$, choose the next rational endpoint so that $K_i^+ < 0$ and $D(t_{i+1} - t_i) \leq -K_i^+/2$, where the rational derivative bound is

$$D = \frac{35046648006}{3000000}.$$

The finite calculation reaches $t_L = 100$ and gives $K_i^+ < 0$ at every left endpoint. Hence $|K'| \leq D$ implies

$$K(t) \leq K_i^+ + D(t - t_i) \leq \frac{K_i^+}{2} < 0 \text{ for } t_i \leq t \leq t_{i+1},$$

so $K(t) < 0$ on $[0, 100]$.

For the large-t estimate, rational lower bounds for the fourth roots give

$$\sum_{q \in \mathcal{Q}} |A_q| q^{-1/4} < 3600.$$

For the other checks involving J_0 on bounded intervals, rational interval evaluation at the grids below give the stated finite bounds. For K_4, the four grid spacings 1/500, 1/100, 1/2000, and 1/100 are used on $[1/10, 1]$, $[1, 3]$, $[3, 4]$, and $[4, 12]$, respectively.

kernel	range	grid spacing	finite bound
H_g	$[0, 25]$	1/400	$H_g(t_j) < 180$
H_s	$[0, 25]$	1/400	$H_s(t_j) < 46019/250$
K_4	$[1/10, 12]$	four spacings above	$K_4(t) < 1991/1000$
K_5	$[0, 12]$	1/200	$K_5(t_j) < 389$

TABLE 3. Finite bounds for the checks involving J_0 on bounded intervals.

The bounds in the table extend to the full intervals by the derivative estimates in the proof sections. The rational interval evaluations use the Bessel-series bound (2.5) and the analogous spherical series estimate in Lemma 10.

kernel	interval	grid spacing	bound at grid points	derivative
H_{34}	$[0, 6]$	$1/5000$	$H_{34}(t_j) < 69/100$	$\lvert H'_{34}\rvert \le 7/2$
H_{35}	$[0, 25]$	$1/2000$	$H_{35}(t_j) < 1469/500$	$\lvert H'_{35}\rvert \le 380/(3\pi) < 95/2$
H_{36}	$[0, 10]$	$1/10000$	$H_{36}(t_j) < 399/1000$	$\lvert H'_{36}\rvert \le 95/8$
H_{44}	$[0, 25]$	$1/2500$	$H_{44}(t_j) < 887/1000$	$\lvert H'_{44}\rvert \le 32/\pi < 12$

TABLE 4. Sample-point bounds and analytic derivative bounds for the four line kernels.

The LPs only choose the coefficients. The proofs use the rounded rational or integer data recorded in Appendix B and the finite arithmetic checks described above.

A.3. **Finite checks for the square–tetrahedron configuration.** The geometric and local counts in Section 9 follow from arithmetic in $\mathbb{Q}(\sqrt{3})$. Represent $a + b\sqrt{3}$ by (a, b), with addition and multiplication given by

$$(a, b) + (c, d) = (a + c, b + d), (a, b)(c, d) = (ac + 3bd, ad + bc).$$

For the labelled points $p_0, \dots, p_{19}$, compute $d_{ij} = |p_i - p_j|^2$. For each $I \in \binom{\{0,\dots,19\}}{4}$, check whether the six values d_{ij} with $i, j \in I$, $i < j$, form the multiset $\{1, 1, 1, 1, 2, 2\}$. If the two pairs with value 2 are disjoint, the subset is a square; if they meet, it is a copy of $\mathcal{T}$. The resulting counts are

quantity	count
distinct points	20
four-point subsets with this distance pattern	46
squares	22
copies of $\mathcal{T}$	24

by Lemma 36.

The group $G = \langle \tau, \sigma \rangle$ has order four. Its action on the unordered pairs is obtained from

$$\mathcal{O}(i, j) = \Big\{\{\min(g(i), g(j)), \max(g(i), g(j))\} : g \in G\Big\},$$

and a calculation gives the following orbit-size distribution:

orbit size	1	2	4	total
number of orbits	2	14	40	56
pairs accounted for	2	28	160	190

The representatives and the associated distances and coefficients are listed in Appendix B.

The local restrictions leave 47946 sign colorings. Substituting the integer coefficients from Appendix B into the local expression gives $1000\mathcal{L}_S \ge 1000$ for each of them.

For the kernel check, use the grid $t_j = j/1000$ on $[0, 40]$. Outward-rounded interval evaluation gives the following upper bounds:

range	interval upper bound
$0 \le t_j < 5$	$3/250$
$5 \le t_j < 10$	-11
$10 \le t_j < 15$	$1/100$
$15 \le t_j < 20$	-17
$20 \le t_j < 25$	-22
$25 \le t_j < 30$	-21
$30 \le t_j < 35$	-22
$35 \le t_j \le 40$	-25

In particular, every sample point satisfies (8.5); the derivative estimate in the proof extends the bound to the intervening intervals.

A.4. **Linear-program sizes.** Table 5 records the dimensions and scalar constraint counts of the nine linear programs. The columns labelled local, kernel, and variable bounds count scalar inequalities; the equality column counts scalar equalities; and total constraints is their sum. A two-sided variable bound contributes two scalar inequalities.

LP	variables	local	kernel	equalities	variable bounds	total constraints
(ℓ_2, ℓ_7)	$172 = 1 + 18 + 153$	751	40001	0	0	40752
(ℓ_2, ℓ_2, ℓ_3)	$31 = 1 + 4 + 13 + 13$	304	20002	0	0	20306
(ℓ_3, ℓ_4)	$11 = 1 + 1 + 2 + 7$	12	30001	1	22	30036
(ℓ_3, ℓ_5)	$49 = 1 + 1 + 6 + 41$	73	50001	1	98	50173
(ℓ_3, ℓ_6)	$50 = 1 + 1 + 5 + 43$	78	100001	1	100	100180
(ℓ_4, ℓ_4)	$19 = 1 + 4 + 14$	26	62501	1	38	62566
$(\ell_2, W_4(\sqrt{2}))$	$38 = 2 + 8 + 28$	37	2126	0	76	2239
(ℓ_2, P_5)	$47 = 2 + 9 + 36$	42	2140	0	94	2276
$\mathcal{S}$–$\mathcal{T}$	$58 = 1 + 1 + 56$	47946	40001	0	114	88061

Table 5. Dimensions and scalar constraints of the nine linear programs.

Appendix B. Coefficient data

This appendix records the coefficient values used in the finite local inequalities. Together with the definitions and finite checks in Appendix A, these data make the finite inequalities independent of the LPs.

The ordering conventions are fixed as follows. In the nine-point configuration, order point labels lexicographically and take the lexicographically least label in each vertex orbit, or the lexicographically least ordered pair in each unordered pair orbit, as its representative; the table rows follow that order. In the eighteen-point configuration, use the point order $00, 01, \ldots, 08, 10, 11, \ldots, 18$; the rows and columns of each coefficient array are indexed by $0, 1, \ldots, 8$, and the squared-distance table is in increasing order. For the square–tetrahedron configuration, the orbit $\mathcal{O}_j$ is the orbit represented in row j of the table below, and that row order defines the indices used in X_j, a_j, and B_q.

B.1. **The nine-point inequality.** The group acting on the nine-point configuration has four vertex orbits and thirteen orbits of unordered pairs. Each pair orbit is determined by the representative in the table by applying the four symmetries of the configuration.

representative	orbit size	coefficient c_O
00	2	−252
01	4	−1004
02	2	998
11	1	−345

Table 6. Nine-point vertex-orbit coefficients.

representative	orbit size	squared distance	a_U	b_U
$00, 01$	4	1	−998	2
$00, 02$	4	4	−1000	0
$00, 11$	2	3	500	150
$00, 12$	4	7	1000	300
$00, 22$	1	12	375	200
$01, 02$	4	1	−446	−894
$01, 10$	2	1	2	502
$01, 11$	4	1	444	948
$01, 12$	2	3	662	−12
$01, 20$	4	3	448	0
$01, 21$	2	4	−264	−12
$02, 11$	2	1	−52	−1000
$02, 20$	1	4	112	0

Table 7. Nine-point pair-orbit coefficients.

B.2. **The eighteen-point inequality.** The first table gives the sum of the pair coefficients at each squared distance. The next table gives the vertex coefficients, followed by the three arrays containing all pair coefficients.

q	1	3	4	7	9	13	16	21	25	31	36	43	49	57	64	73
multiplicity m_q	33	15	14	13	12	11	10	9	8	7	6	5	4	3	2	1
coefficient sum A_q	−489	1035	−669	600	−700	548	−355	441	−105	339	−114	−139	16	−90	0	0

Table 8. The squared-distance multiplicities and aggregated pair coefficients.

The vertex coefficients are

p	00	01	02	03	04	05	06	07	08
c_p	0	−54	−54	−16	−2	15	−46	−1	26
p	10	11	12	13	14	15	16	17	18
c_p	18	−16	−52	1	−18	−23	−44	−53	0

For the pair coefficients, write

$$a^{00}_{jk} = a_{(0,j),(0,k)},$$
$$a^{11}_{jk} = a_{(1,j),(1,k)},$$
$$a^{01}_{jk} = a_{(0,j),(1,k)}.$$

The two within-column upper-triangular arrays and the cross-column array are as follows. A dash denotes an unused diagonal or lower-triangular entry.

$j\backslash k$	0	1	2	3	4	5	6	7	8
0	–	-100	0	0	0	0	0	0	0
1	–	–	-100	-2	-11	-12	14	-16	11
2	–	–	–	-100	-54	-100	-58	-22	-43
3	–	–	–	–	-100	-95	-100	-60	-55
4	–	–	–	–	–	-100	-87	-92	-58
5	–	–	–	–	–	–	-100	-63	-58
6	–	–	–	–	–	–	–	-100	-42
7	–	–	–	–	–	–	–	–	100
8	–	–	–	–	–	–	–	–	–

Table 9. The coefficients a^{00}_{jk} for pairs in the first column.

$j\backslash k$	0	1	2	3	4	5	6	7	8
0	–	100	-38	-52	-52	-49	-43	5	0
1	–	–	100	-57	-77	-46	-13	-12	0
2	–	–	–	100	-77	-100	-57	20	0
3	–	–	–	–	100	-95	-100	-12	0
4	–	–	–	–	–	100	-60	-10	0
5	–	–	–	–	–	–	100	1	0
6	–	–	–	–	–	–	–	100	0
7	–	–	–	–	–	–	–	–	100
8	–	–	–	–	–	–	–	–	–

Table 10. The coefficients a^{11}_{jk} for pairs in the second column.

$j\backslash k$	0	1	2	3	4	5	6	7	8
0	-100	0	0	0	0	0	0	0	0
1	-100	-100	40	14	31	30	57	26	0
2	77	-100	-100	99	78	79	100	59	0
3	63	85	-100	-100	93	67	68	26	0
4	63	57	100	-100	-100	84	56	28	0
5	52	61	65	70	-100	-100	85	7	0
6	67	96	100	73	100	-89	100	39	0
7	-85	93	90	58	60	88	100	100	0
8	-90	-80	63	47	60	60	75	100	100

Table 11. The coefficients a^{01}_{jk} for pairs between the two columns.

B.3. **The pentagon inequality.** The point labels are ordered as in the finite pentagon configuration in the main text. The linear coefficient vector is

$$(\alpha_0, \dots, \alpha_8) = (-23, 77, -100, -23, -23, 100, 100, 100, 77).$$

The nonzero pair coefficients are given by the following upper-triangular matrix; blank entries are zero.

$i\backslash j$	0	1	2	3	4	5	6	7	8
0		-100	23	23	-100	0	0	0	23
1			-100	23	23	-100	-100	-100	-100
2				-100	23	77	-100	77	100
3					-100	0	0	-100	23
4						0	0	0	-100
5							-100	-100	-100
6								-48	-100
7									100
8									

Table 12. Pair coefficients for the finite pentagon inequality.

B.4. **The four line inequalities.** The sequence labels in the following tables are binary. For ϕ_{34}, ϕ_{35}, and ϕ_{36} they are the values of the red indicator r_j. For ϕ_{44}, they are the values $\epsilon_j = r_j = (s_j + 1)/2$; when the local weight is evaluated, the same sequence is converted to signed values by $s_j = 2\epsilon_j - 1$. Thus the listed table omits the forbidden sequences, and no other sequence is part of the domain of a potential.

The two short tables of potential values are

sequence	000	001	010	011	100	101	110
ϕ_{34}	0	−1	−2	−2	−3	−3	−3

Table 13. Potential values for the (ℓ_3, ℓ_4) inequality.

seq.	ϕ_{44}	seq.	ϕ_{44}	seq.	ϕ_{44}	seq.	ϕ_{44}
0001	0	0010	−8	0011	−10	0100	−12
0101	−14	0110	−14	0111	−12	1000	−12
1001	−14	1010	−14	1011	−12	1100	−10
1101	−8	1110	0				

Table 14. Potential values for the (ℓ_4, ℓ_4) inequality.

The two longer tables of potential values follow.

sequence	ϕ_{35}	sequence	ϕ_{35}
000010	−2	000011	0
000100	−8	000101	−8
000110	−6	001000	−14
001001	−14	001010	−14
001011	−14	001100	−13
001101	−12	010000	−20
010001	−20	010010	−20
010011	−20	010100	−22
010101	−20	010110	−20
011000	−24	011001	−22
011010	−20	011011	−18
100001	−26	100010	−26
100011	−26	100100	−30
100101	−28	100110	−28
101000	−28	101001	−28
101010	−26	101011	−26
101100	−29	101101	−27
110000	−30	110001	−30
110010	−28	110011	−28
110100	−26	110101	−26
110110	−24		

Table 15. Potential values for the (ℓ_3, ℓ_5) inequality.

sequence	ϕ_{36}	sequence	ϕ_{36}
000001	0	000010	−2
000011	−2	000100	−4
000101	−4	000110	−4
001000	−6	001001	−6
001010	−6	001011	−6
001100	−6	001101	−6
010000	−8	010001	−8
010010	−8	010011	−8
010100	−9	010101	−8
010110	−9	011000	−8
011001	−8	011010	−8
011011	−8	100000	−10
100001	−10	100010	−11
100011	−10	100100	−12
100101	−11	100110	−13
101000	−11	101001	−11
101010	−11	101011	−10
101100	−12	101101	−11
110000	−10	110001	−10
110010	−10	110011	−10
110100	−10	110101	−10
110110	−10		

Table 16. Potential values for the (ℓ_3, ℓ_6) inequality.

B.5. **The twenty-point square–tetrahedron inequality.** For each row, the representative is a pair of point labels from the square–tetrahedron section. The third column is the size of its orbit under the group G, the fourth is the common squared distance, and the last is the coefficient a_j in the square–tetrahedron expression.

q	B_q	q	B_q
$2-\sqrt{3}$	-68300	1	-300708
$3-\sqrt{3}$	56588	2	-142872
$4-\sqrt{3}$	-14632	3	18334
$5-\sqrt{3}$	10996	$2+\sqrt{3}$	628
4	-5700	$3+\sqrt{3}$	-404
$4+\sqrt{3}$	204	6	386
$5+\sqrt{3}$	380	7	136

Table 17. Aggregated squared-distance coefficients for the square–tetrahedron kernel.

Table 18. The integer pair-orbit data for the square–tetrahedron result.

j	representative	$\lvert\mathcal{O}_j\rvert$	q_j	a_j
0	$\{8,10\}$	4	1	0
1	$\{0,8\}$	4	1	-17344
2	$\{0,10\}$	2	2	-152
3	$\{0,1\}$	4	1	-9839
4	$\{4,8\}$	4	2	-21087
5	$\{0,2\}$	4	1	-10680
6	$\{4,10\}$	2	3	587
7	$\{0,3\}$	4	2	-2319
8	$\{3,4\}$	4	3	2040
9	$\{1,4\}$	4	2	-553
10	$\{1,3\}$	4	1	3317
11	$\{2,3\}$	4	1	-997
12	$\{7,9\}$	4	$3-\sqrt{3}$	5100
13	$\{0,4\}$	1	1	-39099
14	$\{5,14\}$	4	4	-1425
15	$\{2,4\}$	4	2	-1277
16	$\{2,14\}$	2	$2+\sqrt{3}$	-12
17	$\{1,14\}$	4	3	1304
18	$\{3,14\}$	4	$4+\sqrt{3}$	51
19	$\{6,14\}$	2	$3+\sqrt{3}$	-22
20	$\{1,9\}$	4	$2-\sqrt{3}$	-6903
21	$\{7,14\}$	4	$5+\sqrt{3}$	95
22	$\{1,2\}$	4	2	-1171
23	$\{5,9\}$	4	$3-\sqrt{3}$	5627
24	$\{1,5\}$	2	1	-6775
25	$\{5,10\}$	4	$3-\sqrt{3}$	485
26	$\{2,5\}$	4	3	1144
27	$\{2,9\}$	4	1	-9068
28	$\{1,8\}$	4	1	-2603
29	$\{3,5\}$	4	2	-2761
30	$\{3,15\}$	4	$4-\sqrt{3}$	-3658
31	$\{1,10\}$	4	$2-\sqrt{3}$	-337
32	$\{3,16\}$	2	6	193
33	$\{7,15\}$	4	$5-\sqrt{3}$	2749
34	$\{7,16\}$	2	7	68
35	$\{2,10\}$	4	$2+\sqrt{3}$	-294
36	$\{3,9\}$	4	$2-\sqrt{3}$	-6010
37	$\{3,7\}$	2	1	-2480
38	$\{9,11\}$	2	3	460
39	$\{5,8\}$	4	2	-5565
40	$\{1,15\}$	2	$2-\sqrt{3}$	-7650
41	$\{6,8\}$	4	$3+\sqrt{3}$	-21
42	$\{7,8\}$	4	$3+\sqrt{3}$	-145
43	$\{10,11\}$	4	2	537
44	$\{2,8\}$	4	$2+\sqrt{3}$	-93
45	$\{3,10\}$	4	2	-59
46	$\{3,6\}$	4	2	1433
47	$\{6,9\}$	4	2	-2065
48	$\{3,8\}$	4	$2+\sqrt{3}$	550
49	$\{5,15\}$	2	$3-\sqrt{3}$	5870
50	$\{6,10\}$	4	$3+\sqrt{3}$	76
51	$\{8,9\}$	2	2	-1510
52	$\{7,10\}$	4	3	-428
53	$\{10,13\}$	1	1	-267
54	$\{2,6\}$	2	1	-54
55	$\{8,11\}$	2	1	-26934

Acknowledgments

This work was completed as part of the REU on Combinatorics, AI, and Algorithms for Real Problems (REU-CAAR) at the University of Maryland. We thank Bill Gasarch for introducing us to this problem and for his guidance, and Charlie Klawitter, Eva Wu, Hridhaan Banerjee, Sandy Yin, Tane Park, and Ishan Kumthekar for helpful discussions. The implementation of the linear programs and other computational components of this work was partially developed with assistance from GPT-5.6 Luna.

References

[1] G. Ambrus and M. Matolcsi, *Density estimates of 1-avoiding sets via higher order correlations*, Discrete Comput. Geom. **67** (2022), no. 4, 1245–1256.

[2] G. Ambrus, A. Csiszárik, M. Matolcsi, D. Varga, and P. Zsámboki, *The density of planar sets avoiding unit distances*, Math. Program. **207** (2024), no. 1–2, 303–327.

[3] A. Arman and S. Tsaturian, *A result in asymmetric Euclidean Ramsey theory*, Discrete Math. **341** (2018), no. 5, 1502–1508.

[4] C. Bachoc, A. Passuello, and A. Thiery, *The density of sets avoiding distance 1 in euclidean space*, Discrete Comput. Geom. **53** (2015), no. 4, 783–808.

[5] K. Cantwell, *Finite Euclidean Ramsey theory*, J. Combin. Theory Ser. A **73** (1996), no. 2, 273–285.

[6] D. Conlon and J. Fox, *Lines in Euclidean Ramsey theory*, Discrete Comput. Geom. **61** (2019), no. 1, 218–225.

[7] D. Conlon and J. Führer, *Non-spherical sets versus lines in Euclidean Ramsey theory*, Canad. Math. Bull. **69** (2026), no. 1, 179–183.

[8] D. Conlon and Y.-H. Wu, *More on lines in Euclidean Ramsey theory*, C. R. Math. Acad. Sci. Paris **361** (2023), 897–901.

[9] G. Csizmadia and G. Tóth, *Note on a Ramsey-type problem in geometry*, J. Combin. Theory Ser. A **65** (1994), no. 2, 302–306.

[10] G. Currier, P. Mody, Z. Xie, and J. Zhang, *Improved bounds for lines and* 1*-separated sets in Euclidean Ramsey theory*, arXiv:2606.17194 [math.CO], 2026.

[11] G. Currier, K. Moore, and C. H. Yip, *Any two-coloring of the plane contains monochromatic 3-term arithmetic progressions*, Combinatorica **44** (2024), no. 6, 1367–1380.

[12] G. Currier, K. Moore, and C. H. Yip, *Avoiding short progressions in Euclidean Ramsey theory*, J. Combin. Theory Ser. A **217** (2026), 106080.

[13] E. DeCorte, F. M. de Oliveira Filho, and F. Vallentin, *Complete positivity and distance-avoiding sets*, Math. Program. **191** (2022), no. 2, 487–558.

[14] F. M. de Oliveira Filho and F. Vallentin, *Fourier analysis, linear programming, and densities of distance avoiding sets in* $\mathbb{R}^n$, J. Eur. Math. Soc. **12** (2010), no. 6, 1417–1428.

[15] P. Diaconis and D. Freedman, *A Dozen de Finetti-Style Results in Search of a Theory*, Ann. Inst. Henri Poincaré Probab. Stat. **23** (1987), no. S2, 397–423.

[16] P. Erdős, R. L. Graham, P. Montgomery, B. L. Rothschild, J. Spencer, and E. G. Straus, *Euclidean Ramsey theorems. I*, J. Combin. Theory Ser. A **14** (1973), no. 3, 341–363.

[17] P. Erdős, R. L. Graham, P. Montgomery, B. L. Rothschild, J. H. Spencer, and E. G. Straus, *Euclidean Ramsey theorems II*, in *Infinite and Finite Sets*, Colloquia Mathematica Societatis János Bolyai, vol. 10, North-Holland, Amsterdam, 1975, pp. 529–557.

[18] P. Erdős, R. L. Graham, P. Montgomery, B. L. Rothschild, J. H. Spencer, and E. G. Straus, *Euclidean Ramsey theorems III*, in *Infinite and Finite Sets*, Colloquia Mathematica Societatis János Bolyai, vol. 10, North-Holland, Amsterdam, 1975, pp. 559–583.

[19] J. Führer and G. Tóth, *Progressions in Euclidean Ramsey theory*, European J. Combin. **125** (2025), 104105.

[20] W. Gasarch, A. Gezalyan, and R. Parker, *Open Problems Column Monochromatic Unit Squares: Exposition and Open Problems*, SIGACT News **56** (2025), no. 3, 38–55, `https://doi.org/10.1145/3767145.3767149`.

[21] L. Iván, *Monochromatic point sets in the plane and in space*, Master's thesis, University of Szeged, 1979.

[22] S. Janson, *New versions of Suen's correlation inequality*, Random Structures Algorithms **13** (1998), no. 3–4, 467–483.

[23] R. Juhász, *Ramsey type theorems in the plane*, J. Combin. Theory Ser. A **27** (1979), no. 2, 152–160.

[24] T. Keleti, M. Matolcsi, F. M. de Oliveira Filho, and I. Z. Ruzsa, *Better bounds for planar sets avoiding unit distances*, Discrete Comput. Geom. **55** (2016), no. 3, 642–661.

[25] L. Moser and W. Moser, *Solution to problem 10*, Canad. Math. Bull. **4** (1961), 187–189.

[26] F. W. J. Olver, A. B. Olde Daalhuis, D. W. Lozier, B. I. Schneider, R. F. Boisvert, C. W. Clark, B. R. Miller, B. V. Saunders, H. S. Cohl, and M. A. McClain, *NIST Digital Library of Mathematical Functions*, `https://dlmf.nist.gov/`, Release 1.2.7 of 2026-06-15.
[27] B. Simon, *Real Analysis: A Comprehensive Course in Analysis, Part 1*, American Mathematical Society, Providence, RI, 2015.
[28] L. A. Székely, *Measurable chromatic number of geometric graphs and sets without some distances in euclidean space*, Combinatorica **4** (1984), no. 2–3, 213–218.
[29] A. D. Szlam, *Monochromatic translates of configurations in the plane*, J. Combin. Theory Ser. A **93** (2001), no. 1, 173–176.
[30] S. Tsaturian, *A Euclidean Ramsey result in the plane*, Electron. J. Comb. **24** (2017), no. 4, Paper No. P4.35, 9 pp.

Oberlin College
Email address: `hoffcryan@gmail.com`

Williams College
Email address: `gh7@williams.edu`

Bard College
Email address: `yy2323@bard.edu`